Universidade de Lisboa

Faculdade de Farmácia

Metabolic characterization of Sarcomas

Mara Santiago Rodrigues

Dissertação de mestrado orientada pelo Professor Doutor Sérgio Jerónimo Rodrigues Dias e coorientada pela Professora Doutora Joana São José Dias Amaral

Mestrado em Ciências Biofarmacêuticas

2022

Universidade de Lisboa

Faculdade de Farmácia

Metabolic characterization of Sarcomas

Mara Santiago Rodrigues

Trabalho final de Mestrado em Ciências Biofarmacêuticas apresentado à Universidade de Lisboa através da Faculdade de Farmácia

Dissertação de mestrado orientada pelo Professor Doutor Sérgio Jerónimo Rodrigues Dias e coorientada pela Professora Doutora Joana São José Dias Amaral

Mestrado em Ciências Biofarmacêuticas

2022

Agradecimentos

A realização desta tese contou com a ajuda e apoio diretos e indiretos de várias pessoas que me acompanharam e apoiaram e às quais não posso deixar de agradecer.

Em primeiro lugar, quero agradecer ao Dr. Sérgio Dias por me ter dado a oportunidade de realizar a tese de mestrado no seu laboratório, por toda a ajuda e por se ter mostrado sempre disponível. Obrigada também à Ana, por sempre me ter acompanhado e ajudado no que lhe pedia. Um obrigada especial ao Diogo e à Daniela que por nada me deixaram desanimar e se mostraram sempre prontos a dar uma mão amiga.

Gostaria também de agradecer a todos os membros do laboratório do Professor Luís Costa, especialmente à Patrícia por toda a ajuda e preocupação que sempre demonstrou. Obrigada também à Inês, à Raquel e ao Rúben.

Ao querido staff do biobanco, a Ângela, a Ionela e a Andreia que tão bem me acolheram e sempre me apoiaram e ajudaram em todos os aspetos que precisava.

Um enorme obrigada à Dra. Iola Duarte pela ajuda e orientação incansável.

Quero agradecer às duas amigas que mais me apoiaram nesta fase, a Carolina e a Mafalda que por nada me deixaram cair e muito me ensinaram.

À minha família por apoiarem e confiarem nas minhas decisões e me darem a liberdade de escolher o meu futuro, lembrando-me sempre que nunca vão deixar de me dar a mão quando for preciso. À minha mãe, ao meu pai e à minha irmã que sempre me mostraram que desistir não é opção. Por me fazerem quem sou. Por me mostrarem que aconteça o que acontecer, há amor.

Por fim, o maior obrigada ao Beni e à Emma por me darem mais uma razão para continuar.

Resumo

Sarcomas são um grupo heterogéneo de tumores malignos com origem na transformação de células mesenquimais nos tecidos conjuntivos. Estes representam menos de 1% dos cancros adultos e abrangem mais de 170 subtipos, dos quais aproximadamente 87% provêm de tecidos moles e 13% do osso.

A carcinogénese depende de alterações metabólicas e apresenta características comuns a um vasto espetro de diferentes cancros, tal como evasão à apoptose, potencial replicativo ilimitado, reprogramação do metabolismo energético, entre outros.

Dois substratos metabólicos comummente utilizados pelas células cancerígenas para satisfazer as exigências biossintéticas e bioenergéticas são a glucose e a glutamina. Uma forma de estudar as características metabólicas dos tumores, incluindo os sarcomas, abrange diversas técnicas que serão descritas nesta Tese. A resultante Metabolómica é uma ampla análise quantitativa e qualitativa do metaboloma e uma das vantagens desta abordagem reside no facto dos metabolitos estarem a jusante de genes, transcrição e proteínas e, portanto, oferecem a representação mais próxima do fenótipo.

Neste projeto, tínhamos como objetivo criar uma coleção de amostras de sarcoma no Biobanco do iMM-CAML, bem como caracterizar metabolicamente estas amostras, utilizando espectroscopia de RMN e avaliação da expressão genética por PCR quantitativo.

Os resultados preliminares obtidos por RMN apresentaram diferenças evidentes entre o tecido tumoral e o tecido saudável adjacente. As amostras tumorais indicaram uma alta atividade glicolítica, apresentando níveis elevados de lactato acompanhados por níveis reduzidos de glucose. Além disso, foram demonstrados níveis elevados de glutamato juntamente com níveis mais baixos de glutamina, o que sugere um metabolismo de glutamina mais elevado nestas amostras. Outras diferenças observadas envolvem níveis de glucose-1-fosfato e UDP-glucose, bem como BCAA, aminoácidos aromáticos e carnosina. No que diz respeito à expressão genética, os resultados obtidos mostraram uma expressão mais elevada de *LDHA*, seguida por *GAPDH* e *ALDOC*. A *GLS2*, envolvida no metabolismo da glutamina, mostra o nível mais baixo de expressão entre os genes avaliados. A continuação da caracterização metabolómica de amostras de STS permitirá o estabelecimento de diferenças discriminativas entre STS e tecido normal, contribuindo para o desenvolvimento de terapias mais eficazes para estes tumores.

Palavras chave: Cancro, sarcoma, metabolómica, remodelação metabolómica

Abstract

Sarcomas are a heterogenous group of malignant tumors that originate from the transformation of mesenchymal cells in connective tissues. These account for less than 1% of adult cancers and encompass over 170 subtypes, of which approximately 87% arise from soft tissue and 13% from bone. Carcinogenesis is dependent on alterations of the metabolic activity and presents certain characteristics common to a wide spectrum of different cancers, such as apoptosis evasion, unlimited replicative potential, reprogramming of energy metabolism, among others. Two metabolic substrates commonly used by cancer cells to meet the biosynthetic and bioenergetic requirements of these cells are glucose and glutamine.
One way to study the metabolic characteristics of tumors, including sarcomas, comprises several techniques that will be described in this thesis. The resulting Metabolomics is a broad quantitative and qualitative analysis of the metabolome and one of the main advantages regarding this approach lies on the fact that metabolites are downstream of genes, transcripts, and proteins and therefore, give the closest representation of the phenotype.

In this project, we aimed to create a collection of sarcoma samples at the biobank of iMM-CAML, as well as metabolically characterize these samples using NMR spectroscopy and evaluation of genetic expression by quantitative PCR.

The preliminary results obtained on 1H NMR profiling of STS displayed evident differences between tumoral tissue and adjacent non-involved healthy tissue. Tumor samples indicated high glycolytic activity by displaying higher levels of lactate alongside lower levels of glucose. Furthermore, increased levels of glutamate were shown together with lower levels of glutamine, which suggests a higher glutamine metabolism in these samples. Other prominent differences observed regard levels of glucose-1-phosphate and UDP-glucose as well as BCAA, aromatic amino acids and carnosine.

Regarding gene expression, results obtained showed a higher expression of *LDHA*, followed by *GAPDH* and *ALDOC*. *GLS2*, involved in glutamine metabolism, shows the lowest level of expression amongst the assessed genes. The extension of metabolomic characterization of STS samples will allow the establishment of discriminative differences between STS and normal tissue, contributing to the development of more effective therapies for these tumors.

Keywords: Cancer, sarcoma, metabolomic, metabolic remodelling

Index

Index of figures

Index of tables

List of abbreviations

1D- One-dimensional
2D- Two-dimensional
ABCB6- ATP Binding Cassette Subfamily B Member 6
ACLY- ATP Citrate Lyase
ADI-PEG20- Pegylated arginine deiminase
ALDOC- Aldolase C, frutose-bisfosfato
ASS1- Argininosuccinate synthetase 1
ATP- Adenosine triphosphate
AXP- Adenine mono/di/tri phosphate
BCAA- Branched chain amino acids
BLAST – Basic Local Alignment Search Tool
CDS- Coding sequence
CHULN-HSM- Centro Hospitalar Universitário Lisboa, Norte- Hospital de Santa Maria
CTC- Circulating tumor cell
ctDNA- Circulating tumor DNA
CTNNB1- Beta-catenin encoding gene
DDLPS- Dedifferentiated liposarcoma
DMSO- Dimethyl sulfoxide
DNA- Deoxyribonucleic acid
ENO1- Enolase 1
FADH2- Dihydroflavine-adenine dinucleotide
FBP1- Fructose-Bisphosphatase 1
FBS- Fetal bovine serum
FC- Fold change
FFPE- Formalin-fixed, paraffin-embedded
G6P- Glucose-6-phosphate
G6PD- Glucose-6-phosphate dehydrogenase
GAPDH- Glyceraldehyde-3-phosphate dehydrogenase
GLUT- Glucose transporter
GLUT1- Glucose transporter 1
Hif-1- Hypoxia inducible factor 1
HK- Hexokinase
GC- Gas chromatography
GDH- Glutamate dehydrogenase
Glc-6-P- Glucose 6-phosphate
Gln- Gutamine
GLS- Glutaminase
GLS1- Glutaminase1
GLS2- Glutaminase2

Glu- Glutamate
GPC- Glycerophosphocholine
GPI- Glucose-6-Phosphate Isomerase
HK1- Hexokinase1
HK2- Hexokinase2
HPLC- High performance liquid chromatography
HSM- Hospital de Santa Maria
IDH1- Isocitrate Dehydrogenase1
IDH2- Isocitrate Dehydrogenase2
LC- Liquid chromatography
LDH- Lactate dehydrogenase
LDHA- Lactate dehydrogenase A
LDHB- Lactate dehydrogenase B
LMS- Leiomyosarcoma
MAPK- Mitogen-activated protein kinase
MCT- Monocarboxylate transporter
MCT1- Monocarboxylate transporter 1
MCT4- Monocarboxylate transporter 4
MCT- Monocarboxylate transporters
MDH2- Malate dehydrogenase 2
MFS- Myxofibrosarcoma
MPNST- Malignant peripheral nerve sheath tumors
MS- Mass spectrometry
MSI- Mass spectrometry imaging
mtDNA- Mitochondrial genome
mTOR- Mammalian target of rapamycin
mTORC1- Mammalian target of rapamycin complex 1 NAD^+- Nicotinamide adenine dinucleotide
NADH- Reduced Nicotinamide Adenine Dinucleotide NADPH- Nicotinamide adenine dinucleotide phosphate
NADPH- Nicotinamide adenine dinucleotide phosphate
NaN_3- Sodium azide
NMR- Nuclear magnetic resonance
NOESY- Nuclear Overhauser enhancement spectroscopy
OS- Osteosarcoma
OXPHOS- Oxidative phosphorylation
P4HA1- Prolyl 4-Hydroxylase Subunit Alpha 1
PBMC- Peripheral blood mononuclear cell
PC- Pyruvate carboxylase
PDC- Pyruvate dehydrogenase complex
PDH- Pyruvate dehydrogenase

PDK1- Pyruvate Dehydrogenase Kinase 1
PFK- Phosphofructokinase
PFK1- Phosphofructokinase-1
PFKFB- 6-phosphofructo-2-kinase/fructose-2,6-bisphosphatase
PGK1- Phosphoglycerate Kinase 1
PGM- Phosphoglucomutase
Phe- PhenylalaninePI- Propidium iodide
PKM2- Pyruvate kinase isozyme M2
PPP- Pentose phosphate pathway
PIN1- Peptidyl-prolyl isomerase, NIMA-interacting 1
PKM2- Pyruvate kinase M2
PPAR- Peroxisome proliferator-activated receptor
PTEN- Phosphatase and tensin homolog
PTNM- Pathological Tumor-Node-Metastasis
qRT-PCR- Real-Time Quantitative Reverse Transcription PCR
RNA- Ribonucleic acid
ROS- Reactive oxygen species
RTK- Receptor tyrosine kinases
SGLT- Sodium-Glucose Linked Transporter
SDH- Succinate dehydrogenase
STC2- Stanniocalcin 2
STS- Soft tissue sarcoma
TCA cycle- Tricarboxylic acid cycle
TOCSY- Total correlation spectroscopy
TP53- Tumor protein p53
Tyr- Tyrosine
UDP-glucose- Uracil-diphosphate glucose
UPS- Undifferentiated pleomorphic sarcoma

1. Introduction

Cancer is the second leading cause of death in the world after cardiovascular diseases[1]. It presents itself as a barrier to increasing life expectancy in every country of the world in the 21st century. Its incidence and mortality are rapidly growing worldwide and it reflects both aging and rapid growth of the population[2].

Cancer is a group of diseases caused by the accumulation of acquired or somatic mutations in the DNA[3]. In non-malignant cells, DNA damage is balanced by multiple pathways for DNA repair, and most damage is repaired without error. However, in cancer cells, damage may overwhelm the repair capacity, resulting in the accumulation of mutations[4]. As a consequence of the DNA damage, deregulation of the pathways that control cell proliferation and survival occurs, leading to unregulated cell proliferation[3].

Cancer cells present characteristic hallmarks such as self-sufficiency in growth signals, insensitivity to anti-growth signals, evading apoptosis, limitless replicative potential, sustained angiogenesis and tissue invasion and metastasis[3]. Two new emerging hallmarks were more recently added to the list, namely reprogramming of energy metabolism and evading immune destruction[5]. An updated list of the Hallmarks of cancer was proposed in 2022, and now includes unlocking phenotypic plasticity, nonmutational epigenetic reprogramming, polymorphic variations in microbiomes and senescent cells of different origin that contribute to the development and progression of cancer[6].

For years, classical therapies included surgical tumor removal and cytotoxic chemotherapy[7]. However, the improvement of knowledge on cancer pathogenesis, allowed the development of targeted, more specific therapies, such as monoclonal antibodies and small molecule inhibitors. The latter are nowadays a crucial component of cancer therapy for various common malignancies such as breast, lung or pancreatic cancer[8]. These targeted therapies are generally better tolerated that traditional chemotherapy however[8], they can still lead to cancer cell resistance, which remains an obstacle to cancer therapy. In terms of drug resistance, it may be intrinsic or acquired. The intrinsic chemoresistance refers to cancer cells that present capacities of drug resistance from the beginning of anti-cancer treatment, including limited drug uptake or activating detoxification of drugs[9]. The mechanism of acquired chemoresistance is based on genetic, epigenetic and metabolic alterations of crucial genes in cancer cells, which occur during treatment, which can induce cells to adapt the apoptotic stress caused by the drug[9].

1.1 Cancer metabolism

A complete carcinogenesis process includes alterations of the metabolic activity to support anabolic growth and maintain malignant properties. A common feature of cancer

metabolism is the capacity to support cell survival in a frequently nutrient-poor environment in order to fulfil the biosynthetic and bioenergetic demands[10].
Exploiting and characterizing reprogrammed activities characteristic of cancer cell metabolism may provide opportunities to improve treatment approaches, but requires defining and understanding the pathways that are involved in limiting cancer progression[11,12].

One of the most studied reprogrammed metabolic pathways in cancer is the Warburg effect or aerobic glycolysis. Under physiological conditions, glycolysis is a response to hypoxia in tissues but, in 1923, Otto Warburg showed that, under aerobic conditions, cancer cells metabolize approximately ten times more glucose into lactate relative to normal tissues. Warburg's studies indicated that the cancer cells used, were exhibiting a reversed Pasteur effect, which stands as the inhibition of fermentation by O_2[11,13].

Warburg's hypothesis that cancer cells present increased aerobic glycolysis often leads to the misconception that these cells rely on glycolysis, rather than oxidative phosphorylation (OXPHOS), as their major source of ATP, as a consequence of damage to mitochondrial respiration[11,13,14]. However, nowadays it is known that many cancer cells exhibit the Warburg effect while retaining mitochondrial respiration in order to fulfil the high demand for anabolic processes[13]. Furthermore, it has been demonstrated that cancer cells present the Warburg effect due to activation of oncogenes, loss of tumor suppressors, and up-regulation of the PI3K pathway[11,13]. The increase in glycolytic flux allows glycolytic intermediates to supply subsidiary biosynthetic pathways to fulfil the metabolic demands of proliferating cells, which benefits cancer progression[11].

Due to the high glycolytic rate, cancer cells exhibit an increased rate of glucose uptake with lactate production through aerobic glycolysis with the production of carbon skeletons, NADPH and ATP. However, limiting glycolytic ATP production by inhibiting the activity of pyruvate kinase fails to prevent tumorigenesis, which suggests that the major role of glycolysis is not to supply ATP. Thus, despite their high glycolytic rates, most cancer cells generate the majority of ATP through mitochondrial function proving that mitochondrial metabolism is necessary for cancer cell proliferation and tumorigenesis[11,12,14].

1.2 Glucose metabolism

In the tumor microenvironment, cells must increase the import of nutrients in order to fulfil the biosynthetic demands associated with the progression of the malignancy. As a result of the latter, cancer cells often encounter nutrient scarce environments, mostly due to the inadequacies of the tumor vascular supply[10]. Therefore, in order to survive in an environment with depleted nutrient supply, cancer cells often acquire the ability to use alternative pathways to obtain the necessary nutrients[10,14].

One of the main metabolic substrates used by cancer cells is glucose, which is a source of energy and an important precursor of amino acids, nucleotide and lipids[10,15]. Glycolysis is the main supplier of biosynthetic pathways needed to sustain the high proliferation rate in cancer cells[16].

Proliferating cells tend to overexpress glucose transporters and glycolytic enzymes in order to power the machinery required to degrade glucose, which is consistent with aerobic glycolysis without loss of respiration[10,12]. The transport of glucose through the plasma membrane into the cytosol is mediated by glucose transporters[15]. There are two classes of the latter: the facilitative glucose transporters (GLUTs) that mediate glucose transportation along the concentration gradient[15], and the Na^+ /glucose cotransporters (SGLT), which transport glucose against the concentration gradient using the electrochemical sodium gradient[17,18]. These transporters control the import and export of glucose to ensure constant availability of glucose to support the metabolic needs of the cell[15].

GLUT1 is one of the most commonly studied glucose transporters due to its high affinity for glucose, having a significant role in tissues that are highly dependent on glucose. It is responsible for basal glucose transport and has been found to be overexpressed in a variety of neoplasias where the level of expression correlates with the metastatic potential[15].

The import of nutrients into a normal cell is not a constitutive process - it is tightly regulated by growth factor signaling. However, cancer cell survival might be challenged by a growth-factor-deprived environment, in which cancer cells must adapt and constitutively take up glucose by expressing GLUT1 and the first enzymes of the glycolytic pathway hexokinase 1/2 (HK 1/2)[10,11,19].

Metabolization of glucose occurs through glycolysis with generation of pyruvate in the cytoplasm, which may follow into the tricarboxylic acid (TCA) cycle to fuel OXPHOS in mitochondria[20,21]. The increased rate of glycolysis in cancer cells prompts the conversion of pyruvate into lactate, since pyruvate cannot accumulate in the cell as it is a cytotoxic alkylating compound and lactate is easily exported to the extracellular medium[16].

1.3 Glutamine metabolism

Glutamine is the most copious amino acid, and highly proliferative cells metabolize it for various purposes such as a source of critical elements, like carbon and nitrogen, to fuel fatty acid synthesis and nucleotide biosynthesis, respectively[22,23]. Glutamine also presents an important role in replenishing intermediates of the TCA cycle and contributing to the maintenance of redox homeostasis[22,24], since it acts as a source of nicotinamide adenine dinucleotide (NADH) and flavin adenine dinucleotide ($FADH_2$)[22,25]. Furthermore, it has been shown that glutamine levels are rate-limiting in regards of cell cycle progression and deficiency of these levels may lead to cell cycle arrest in S phase[25].

Glutaminase (GLS) catalyzes the conversion of glutamine to glutamate and this rate-limiting enzyme exists in two isoforms, glutaminase 1 (GLS1) and 2 (GLS2). Glutamate can also act as a source of nitrogen for the synthesis of nonessential amino acids via transamination[22,25].

It is known that most proliferating cells rely on an exogenous glutamine source[25], however, various studies on glutamine deprivation or inhibition of its catabolism have demonstrated that certain cell types present the ability to thrive in the absence of this amino acid, which

suggests intracellular *de novo* glutamine synthesis. In fact, overexpression of glutamine synthase has been found in come cancer types[24,25].

Although not much is known regarding the influence of this amino acid in STS, given the importance of glutamine in supporting bioenergetics and biosynthesis of highly proliferative cells, targeting its metabolism presents as a potential therapeutic option in various cancer subtypes, including sarcoma[22,23].

1.4 Mitochondrial metabolism

Mitochondria are crucial in cancer metabolism and, unlike what was originally thought, functional mitochondria are essential for cancer cells[26,27]. These organelles are involved in many crucial cellular parameters such as regulation of energy production, generation of ROS, modulation of the redox status and initiation of apoptosis[26]. Furthermore, mitochondria are significantly involved in cancer metabolic reprogramming due to the fact that most metabolic pathways, including biosynthesis of nucleic acids, lipids and amino acids, converge into the mitochondria[26,27].

Mutations in the mitochondrial genome (mtDNA) or mitochondrial enzyme defects are common in cancer cells, which leads to mitochondrial dysfunction[27,28]. Moreover, it has been shown that tumor-initiating cells, thought to be involved in cancer recurrence after chemotherapy present reduced mtDNA content[27]. However, instead of inactivating mitochondrial energy metabolism and function, these mitochondrial defects alter the bioenergetic and biosynthetic state of cancer cells, leading to the activation of cytosolic signaling pathways that ultimately alter the activity of cancer- related genes, a process called retrograde signaling[26–28].

Cancer cell defects in mitochondrial enzymes such as succinate dehydrogenase (SDH), malate dehydrogenase 2 (MDH2) and isocitrate dehydrogenase 1 (IDH1) and IDH2 have been established and are linked with familial and sporadic forms of cancer[26,28]. Additionally, it has been shown that altered oncogenes and tumor suppressors such as hypoxia-inducible factor 1 (HIF-1) and tumor suppressor p53 (TP53) are involved in the regulation of mitochondrial respiration and cellular metabolism through modulation of the expression of their target genes[28].

The various functions of mitochondria contribute to cell adaptation when facing challenging microenvironment conditions, and defects in these organelles lead to the initiation of a complex cellular reprogramming that confers a high degree of plasticity to tumor cells, supporting growth and progression of cancers[27,28].

1.5 Metabolic reprogramming

Cancer cells uptake increased amounts of glucose and glutamine which are used to fuel several anabolic pathways, including the TCA cycle, OXPHOS, the pentose phosphate pathway for nucleotide synthesis, and the synthesis of amino acids and lipids, accounting for cell proliferation[21]. These metabolic programs offer both energy and vital precursors to

sustain large-scale biosynthesis and support continuous proliferation, tissue invasion, metastasis, survival and resistance to therapies[29]. Glucose metabolism is enhanced in cancer cells by favored expression of glucose transporters (GLUTs) which mediate the uptake of glucose and are known to be deregulated in cancer[14,20].

Glucose is converted to glucose-6-phosphate (G6P) by hexokinase 2 (HK2), which stands as the first rate-limiting enzyme in glycolysis and is also known to be overexpressed in cancer cells[14]. G6P enters the PPP pathway to supply nucleotides and amino acids syntheses, needed to sustain proliferation. PPP activation induces nicotinamide adenine dinucleotide phosphate (NADPH) which can provide substrates for lipid metabolism and nucleic acid metabolism. Moreover, NADPH is used to maintain antioxidant capacity[11,14].

Pyruvate produced through the glycolytic pathway provides lactate by the action of lactate dehydrogenase A (LDHA) or can be decarboxylated into acetyl-CoA by pyruvate dehydrogenase (PDH) and carboxylated into oxaloacetate by pyruvate carboxylase (PC). The latter are transported to the mitochondria to fuel the TCA cycle[11,30].

Cells export and import lactate through MCTs in a system known as the lactate shuttle. Higher levels of monocarboxylate transporters (MCTs) were found in cancer cells, which are responsible, not only for the high lactate flux, but also for maintaining appropriate intracellular pH, which allows glycolysis to continue. Citrate, a TCA cycle intermediate, is used to generate cytosolic acetyl-CoA for lipid synthesis[14,21,30].

Cancer cells have increased generation of reactive oxygen species (ROS), which demands appropriate level of antioxidants in order to maintain redox balance. Cells can prevent the build-up of ROS by increasing antioxidant capacity such as the use of PPP to generate NADPH, in abundant glucose conditions or reducing glutathione, under the action of glutathione reductase, using NADPH derived from the PPP[11,21].

Furthermore, cancer cells have aberrant activation of the PI3K/AKT/mTOR pathway, which induces anabolic growth. The latter receives extracellular RTK signals, such as growth factors, that activate intra-cellular PI3K signals, which consequently activate the AKT structure. AKT activates mTOR that regulates numerous downstream factors[11,30].

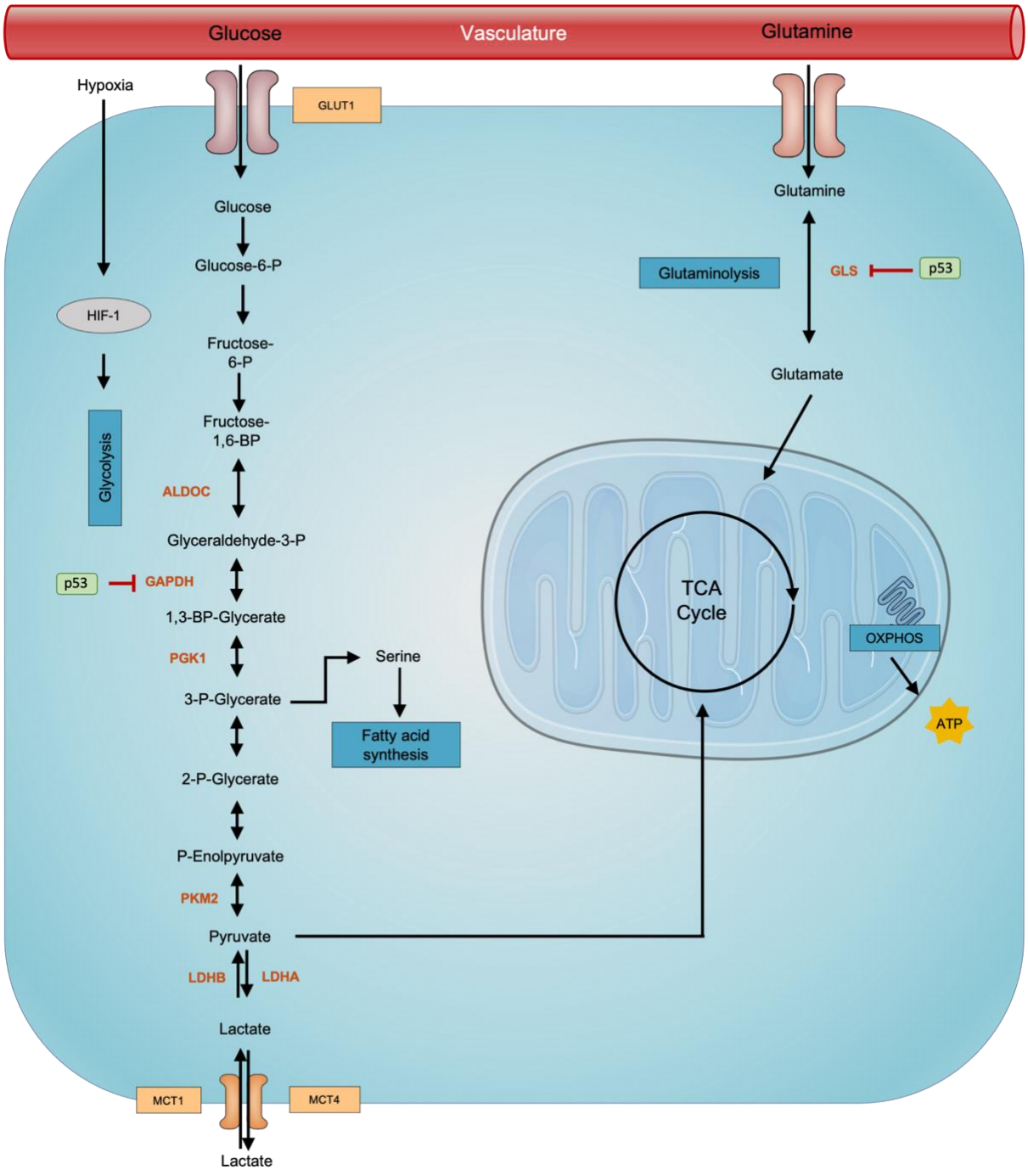

Fig. 1- Metabolic alterations associated with STS. This scheme depicts some known metabolic alterations in sarcoma with emphasis on glycolysis and glutamine metabolism.

1.6 Sarcoma

Sarcomas are a heterogenous group of malignant tumors that originate from the malignant transformation of mesenchymal cells in connective tissues. These present as an aggressive disease with a late diagnosis on most cases[31]. Sarcomas account for less than 1% of adult cancers and around 15% of pediatric cancers. These encompass over 170 subtypes, of which approximately 87% arise from soft tissue and 13% from bone[23]. Prognosis is rather dismal and current classification approaches rely on histopathological criteria, which leads to errors in approximately 25% of cases[25,32]. Currently, only 50% of sarcoma patients are treated accordingly with their specific subtype, and the 5-year survival rate of patients with metastatic disease is only 16%. Treatment options are scarce, with surgery being the standard option alongside with chemotherapy and radiotherapy[25,33].

1.7 Soft tissue sarcoma metabolomics

In 2017, Abeshouse et al. proposed a new classification of soft tissue sarcomas (STS) subtypes with particular complex genomes by combining genetic, epigenetic and transcriptomic analyses. As a result of the latter, they identified three new dominant profiles from leiomyosarcoma (LMS), myxofibrosarcoma (MFS), undifferentiated pleomorphic sarcoma (UPS) to dedifferentiated liposarcoma (DDLPS)[34].

When considering individual signatures of an STS subtype, such as UPS, an enrichment in PPAR/fatty acids and glycine/serine/threonine pathways lights up, while analyzing LMS, the latter displays and enhanced OXPHOS signature. When evaluating the contribution of different metabolic pathways to sarcomagenesis in STS as a whole, pathways such as RAS, PI3K and HIPPO as well as glycolysis/OXPHOS are highlighted[31].

Hyperactivation of Ras and PI3K pathways drives an upregulation of glucose importers (GLUT) and upstream glycolytic enzymes such as hexokinase (HK), consequently driving a Warburg effect in sarcomas[31]. Furthermore, hyperactivation of Ras pathway has shown to modulate the activity of PKM2 and PGK1, two enzymes involved in the glycolysis pathway, by enabling these with oncogenic functions[35]. Lastly, it has been shown that hyperactivation of the Ras pathway, alongside loss of PTEN, stimulates autonomous nutrient uptake in LMS and supports UPS progression[31,36].

Regarding ERK, a study showed that its activation phosphorylates PGK1 and promotes its association with PIN1 and consequent translocation to the mitochondria. Afterwards, pyruvate dehydrogenase kinase 1 (PDK1) is activated[37]. The latter is an inhibitor of pyruvate dehydrogenase (PDH), the checkpoint of pyruvate entry in the TCA cycle[31].

When taking into consideration all these RAS-driven consequences, it's possible to assess that its alteration supports glucose and glutamine-dependent anabolism over mitochondrial respiration[31].

Mutations related to the constituents of the HIPPO pathway are also related to augmented aerobic glycolysis in STS[31].

Regarding glutamine metabolism, STS usually display enhanced glutamine uptake as well as high glutaminase expression[22] and an elevated reliance on arginine, with a protein arginine methyltransferase overexpression[38].
Currently, the are several ongoing trials experimenting drug inhibition of PI3K, AKT, mTOR and ERK signaling in STS[33].

1.8 Metabolomic approaches for sarcomas

Metabolomics presents as a broad quantitative and qualitative analysis of the metabolome. One of the main advantages regarding this approach lies on the fact that metabolites are downstream of genes, transcripts, and proteins, and therefore any alterations in these will be perceived, giving the closest representation of the phenotype[39].

Metabolomic analysis is usually performed either by targeted or untargeted approaches, however, both methods require identification and quantification of metabolites[40]. Regarding untargeted approaches, such as metabolite profiling and metabolic fingerprinting, an assessment of all available metabolites in a sample is performed and the latter are measured and compared. Later on, some of these signals are assigned their metabolite ID with the assistance of metabolomics databases[40,41]. Unfortunately, a substantial amount of signals detected by this approach, still can´t be identified due to the lack of spectra information in the available databases[40]. The most frequently applied method is metabolite profiling, which analyses a set of known and unknown metabolites based on their chemical nature[41].

Targeted or semi-targeted approaches are based on the identification and quantification of a previously established group of metabolites[40,41]. This technique highly contributes to the unravelling of metabolic differences between groups[41].

Regarding data acquisition methods, mass spectrometry (MS) and nuclear magnetic resonance (NMR) spectroscopy are the most frequently employed techniques[41,42].

1.8.1 NMR

NMR spectroscopy is one of the major contributors in the growing field of metabolomics. It is a quantitative high-throughput technology that allows the identification of small biomolecules based on the magnetic properties of the atomic nuclei[43].

In metabolomics, numerous active nuclei, such as ^{1}H,^{13}C, ^{31}P and ^{15}N , can be used to analyze metabolites present in biological mixtures and although it is a less sensitive technique when compared to mass spectrometry, it holds numerous benefits including the fact that it is highly reproducible and quantitative, non-destructive and non-invasive, and allows for the identification of unknown metabolites as well as the tracing of metabolic pathways and

downstream products of isotope labeled precursors[42,43]. Also, NMR spectroscopy does not require any prior sample preparation or separation, thus reducing analytical variability.

Conversely, this technique presents low sensitivity when comparing to MS and upon analysis of complex samples such as blood, signal overlaps may occur. Also, it fails to detect low abundance metabolites[42,43].

One-dimensional (1D) experiments, such as NOESY (nuclear Overhauser enhancement spectroscopy), are the most commonly used due to the ease of use and high-throughput[42]. Two-dimensional (2D) NMR experiments, such as correlation spectroscopy (COSY) and total correlation spectroscopy (TOCSY), currently represent a great alternative for the identification of unknown metabolites. These experiments improve the spectral resolution and alleviate the peak overlap problem for complex biological samples, contributing to a significantly improved quantitation[42].

A study, by Kelly A. Mercier et al., on desmoid tumors, aimed to understand the metabolomic differences between paired normal fibroblast and desmoid cells from affected patients and normal fibroblasts from unaffected patients[44]. Desmoid tumors are locally invasive soft tissue tumors that lack the ability to metastasize and are often related to T41A and S45F mutations of the beta-catenin encoding gene (*CTNNB1*). Using broad spectrum metabolomics the authors revealed different metabolic profiles of the two beta-catenin mutations and, upon treatment with two drugs, (Dasatinib and FAK) the results showed distinct metabolic profiles for the normal fibroblast and desmoid tumor cells.

1.8.2 MS

Mass spectrometry, another major contributor to the field of metabolomics, is a highly sensitive technique that enables the analysis, identification and quantification of several hundreds to thousands of metabolites[41,42]. Unlike NMR spectroscopy, this technique is generally coupled with chromatographic techniques, such as liquid chromatography (LC), gas chromatography (GC) or electrophoresis that allow the separation of compounds from a complex mixture, prior to detection[41,42].

Some of the most significant advantages this technique presents are its high sensitivity and specificity, as well as the possibility of identification of unknown metabolites[41,45]. When compared to NMR spectroscopy, this technique presents some advantages such as low sample volumes, low cost and the possibility of compound separation prior to MS acquisition. Upon combination of MS with prior chromatographic techniques, the capability of quantitative analysis of complex biological samples significantly increases[43,45].

Regarding liquid chromatography, modern techniques like high-performance liquid chromatography (HPLC) have shown significant improvement in the chromatographic separation, improving resolution when compared to the standard LC techniques[41,45]. Andrew D. Kelly et al. presented the analysis of metabolites extracted from formalin-fixed, paraffin-embedded (FFPE) specimens, using targeted liquid chromatography- tandem mass

spectrometry (LC/MS/MS)[46]. In this study, the authors used soft tissue sarcomas paired with normal samples, and demonstrated excellent reproducibility and correlation between different sections of the same specimen, validating that consistent and reliable data may be acquired from FFPE STS samples using this technique. The authors observed a mean value of 106 metabolites robustly detected throughout the samples, with a trend towards higher metabolite detection rates in the tumor samples.

Pearl Lee et al., used a combination of LC-MS and stable isotope metabolite tracing to demonstrate that cancer cells from an undifferentiated pleomorphic sarcoma (UPS) mouse model were relying on glutaminolysis, opposing with muscle cells[22]. In this model, glutamine presented as a donor for the TCA cycle and a nitrogen donor for aspartate production from oxaloacetate.

Gas chromatography is another metabolite separation technique that can be combined with MS (GC/MS)[33]. However, the latter can only cope with volatile metabolites, therefore, these metabolites have to be derivatized. This presents as a disadvantage of GC/MS, since this modification will interfere with metabolite structure and subsequent identification[31,43].

Although LC/MS holds a wider range of detectable metabolites, GC/MS allows a better compound identification when compared with the first[43].

1.8.3 MSI

Mass spectrometry imaging (MSI) is a method that enables the direct visualization and differentiation of tissue regions based on their metabolic content. It requires no labeling and allows the obtention of tumor-specific molecular signatures regarding the patient's histopathologic context[41,47]. Sha Lou et al., used this method to identify prognostic metabolite biomarkers in high grade sarcomas (osteosarcoma, leiomyosarcoma, myxofibrosarcoma, and undifferentiated pleomorphic sarcoma) using fresh frozen tumor tissues[47]. Of all the metabolites, they noticed inositol cyclic phosphate was correlating with overall survival and carnitine was correlating with metastasis-free survival. Therefore, both these metabolites present as potential prognostic biomarkers in soft tissue sarcoma patients.

Recent progress in data acquisition and processing methods has contributed impressively to the latest advances in unraveling STS features. More refined techniques such as Ultra High-Performance Liquid Chromatography Q-Exactive MS (UHPLC-QE MS) have permitted the detection of a vast spectrum of metabolites, while saving time in sample preparation. Regarding NMR, custom-made NMR detectors integrated with microfluids have shown to provide real-time and dynamic information on the metabolism of 3D tumor spheroids[48,49]. An adaptation of the latter to STS could contribute tremendously to the understanding of its malignant properties, and consequently, to STS metabolic landscape mapping.

2. Aims of the project

The first aim of this project is to create a sarcoma sample collection at the iMM-biobank to be used now, as well as in future studies. This collection includes blood samples as well as tissue samples obtained from patients that have their sarcoma surgically resected in CHULN-HSM. The second aim is to metabolically characterize these tumors, in order to deepen sarcoma metabolomic knowledge, allowing the identification of new potential diagnostic and therapeutic targets.

Improving current knowledge on sarcoma metabolomic is crucial to find potential diagnostic and therapeutic targets and given the limits of current treatments, exploiting metabolic pathways may provide insight into effective therapy for this disease.

3. Materials and methods

3.1 Sarcoma samples: creation of a Biobank Circuit

Patients included in this study were >/= 18 years-old, had an established diagnosis of sarcoma, and were not submitted to any type of neoadjuvant therapy. Primary tumors were surgically resected and patients are followed-up in the medical oncology and/or orthopedics and/or general surgery outpatient clinics of CHULN-HSM. Metastasis samples were also obtained. These samples were subsequently transported and stored at the iMM- Biobank, being included in the sarcoma collection being created.

To operationalize tissue collection, transport, and storage and to optimize the timings involved, a sarcoma sample circuit was created in November 2021. This circuit is currently active and being used. 11 samples have already been collected and stored at the iMM Biobank sarcoma collection.

The circuit includes 4 different steps, the first one involving the explanation of the study to the patient and informed consent. The second step takes place at the operating room and comprises the collection of the blood samples (5 EDTA tubes and 1 serum tube), which are immediately transported by the iMM- Biobank staff to the Biobank, and where the surgical specimen is collected and transported in less than 30 mins to the pathology department for analysis and processing. The third step involves the analysis of the specimen and collection of tumoral and healthy tissue (around 50mg, each), which are posteriorly snap-frozen and stored at the Biobank. The pathology team completes the remaining information fields (fields relative to the time of sample congelation, organ and topography origin, dimension of the surgical specimen, tumor size, type of tissue, collection, and conservation, number of fragments, existence of paraffin-embedded tissue, histopathological diagnosis and grade, pTNM staging, and, regarding paraffin-embedded sample characteristics, particular data and specifications). The fourth step takes place at the iMM-Biobank and encompasses the processing of both the blood and tissue samples and storage of these in liquid nitrogen (at -196°C).

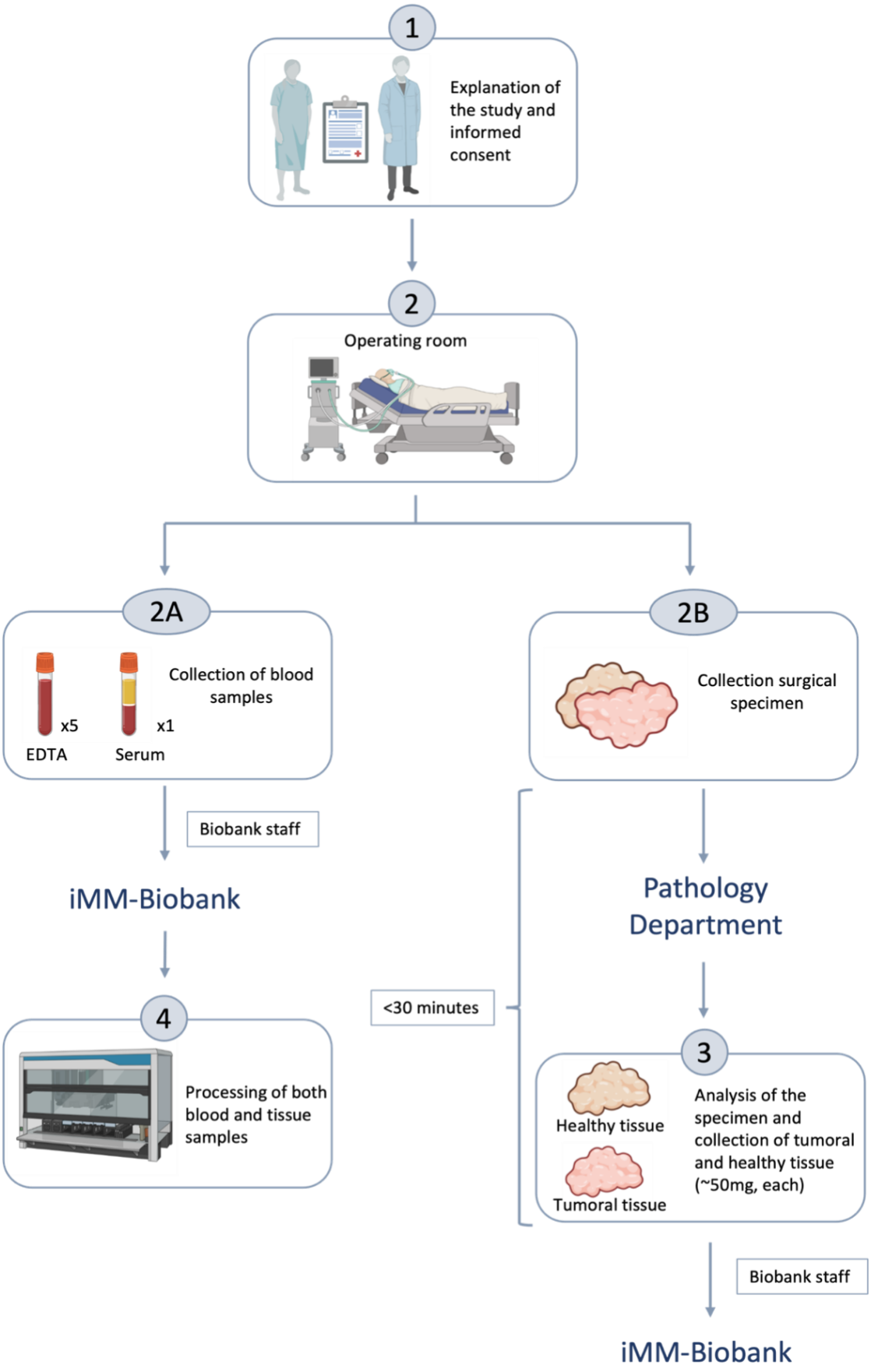

Fig. 2-Schematic representation of the established circuit for the creation of a Sarcoma sample collection at iMM-Biobank

3.2 Processing of blood samples

- Isolation of PBMCs (peripheral blood mononuclear cells)

Each sample was separately processed. Blood samples were first diluted in PBS (gibco, pH 7.4, 1x) in a 1:1 ratio. 15 mL falcon tubes were used and 5 mL of Ficoll-Paque (room temperature, Cytiva) was added to each tube. Approximately 8 mL of diluted blood was carefully added on top of Ficoll-Paque in each tube, creating a density gradient. Samples were centrifuged at 750 x g for 20 mins at 22°C. The obtained cell rings were transferred to new falcon tubes and these were filled with PBS (1x, sterile). Samples were again centrifuged at 540 x g for 10 mins at 22°C. The supernatant was discarded, the pellet was resuspended and the tube was filled with PBS (1x, sterile). The samples were centrifuged at 200 x g for 10 mins at 22°C. The supernatant was discarded and all pellets were transferred to 1 single falcon tube and 10 mL of PBS (1x, sterile) was added. An aliquot of 10 µL was separated for posterior cell counting. Samples were centrifuged at 200 x g for 10 mins at 22°C. Cell counting was performed using 10 µL of cell solution and 90 µL of acetic acid (2%) and according to the number of cells, the pellet was resuspended in cold, inactivated fetal bovine serum (FBS, sigma- aldrich). A DNA pellet corresponding to ~ $1x10^6$ cells was stored at -20°C. Regarding PBMCs, 500 µL aliquots of the sample were distributed in cryotubes, and 500 µL of freezy mix (80% FBS e 20% DMSO (sigma)) was added. The cryotubes were placed in a cell freezing container and stored at -80°C for 48h and posteriorly transferred to a liquid nitrogen container for long-term storage.

- Serum separation

To recover serum from the blood samples, these had to be collected in tubes without anticoagulant. The collection tubes were centrifuged at 2000 x g for 10 mins at room temperature, which enables a serum separation. Serum was then recovered with micropipette and disposable tips and approximately 6 250 µL aliquots were placed in 2 mL cryotubes. Freezing process was gradual and samples were stored at -80°C.

3.3 NMR

3.3.1 Metabolite extraction for NMR analysis

For metabolite extraction, approximately 50 mg of tissue previously collected from patients was macerated in an Agate mortar with pestle, using liquid nitrogen and placed on top of dry ice. The macerated tissue was then weighted again to assess the final weight, since part of the sample might have been lost in the maceration process. After that, cold PBS (gibco, 100 mM, pH7.4) was added in a proportion of 1 mL buffer to 50 mg of tissue. Metabolite

extraction was performed by adding 2 mL of ice-cold methanol 100% (VWR chemicals), followed by the addition of 2 mL of ice-cold chloroform (merck) and 0.5 mL of milliQ water. The aqueous phase and organic phase were separated and divided in aliquots. The organic phase (lipidic fraction) was evaporated under a nitrogen stream and suspended in deuterated chloroform, and the aqueous phase supernatants were dried in a vacuum concentrator (Speedvac, savant) and suspended in phosphate buffer (0.35 mol/L, pH 7.0 in 99.8% D2O containing 2 mmol/L NaN_3) upon sample preparation for NMR analysis. After metabolite extraction, samples were sent to CICECO- Aveiro for NMR analysis.

3.3.2 Acquisition of NMR spectra

1H NMR spectra were acquired at 25°C in a Avance III HD 500 spectrometer (UA, PT NMR Network), 500.13 MHz, Triple Resonance probe (TXI). For the aqueous extracts one-dimensional 1H-NMR spectra were acquired using the NOESY1D pulse sequence with optimized water presaturation (noesygppr1d from Bruker library), as a sum of 512 scans, 2 s relaxation delay, 100 ms mixing time, 32 k points, sw 16 ppm. The organic extracts were acquired using a simple pulse-acquire sequence (zg, from Bruker library), 512 scans, 2 s relaxation delay, 100 ms mixing time, 32 k points, sw 16 ppm. The spectra were manually phased, baseline-corrected and internally referenced to the chemical shift of alanine methyl protons (resonating at 1.47 ppm, for aqueous extracts) or to the residual signal of chloroform (resonating at 7.24 ppm, for the lipidic extracts). Statistical data analysis was performed using R statistical software (https://www.r-project.org/). Metabolite identification was performed by comparison with pure compound spectra from to the Human Metabolome database (http://www.hmdb.ca),and confirmed through 2D- NMR experiments (H-H TOCSY, H-C HSQC and H-J-Resolved).

3.4 RNA extraction, reverse transcription (RT) and relative quantifying real-time polymerase chain reaction (RQ-PCR)

3.4.1 Primer design

The aim of this project was to study gene expression of genes involved in glucose metabolism (*LDHA, ALDOC, GAPDH, PGK1*), glutamine metabolism (*GLS2*) and also mitochondrial metabolism (*MDH2*). The primers LDHA and GLS2 were already available at the lab, however, primers to the genes *ALDOC, GAPDH, PGK1* and *MDH2* were designed using Primer3 (https://primer3.ut.ee). First, the coding sequence (CDS) of the gene of interest was acquired at NCBI- Nucleotide (https://www.ncbi.nlm.nih.gov/nucleotide/). The CDS was then inserted on Primer3 and 4/5 pairs of primers were obtained. After this, a BLAST search was applied to each of the sequences suggested, and the sequence with higher specificity to the gene/transcript of interest and lowest E value was chosen and primers were acquired.

3.4.2 RNA extraction

RNA was extracted from 25 formalin fixed paraffin embedded (FFPE) sarcoma tissue samples, using the PureLink FFPE Total RNA Isolation Kit (Invitrogen). 30 µm sections of tissue samples were placed into a sterile, RNAse-free 1.5 mL microcentrifuge tube and 300 µL of melting buffer were added. Samples were centrifuged for 20 seconds at maximum speed (17000 x g) and afterwards were incubated for 10 mins at 72°C with intermittent gentle mixing every 2-3 mins to melt the paraffin. 20 µL of proteinase K was added and the sample mixed well by pipetting up and down. Samples were incubated at 60°C for 60 mins with occasional mixing and then centrifuged at 17000 x g for 1 min to form a thin layer of paraffin at the top. Using a pipette tip, the solution containing the tissue lysate was aspirated and transferred to a clean RNase-free tube. Afterwards, 400 µL of binding buffer and 800 µL 100% ethanol (sigma- aldrich) were added and samples were vortexed. 700 µL of the latter was transferred to the Spin Cartridge in a collection tube and centrifuged at 800 x g for 1 min. Flowthrough was discarded, the remaining sample was added to the Spin Cartridge and centrifuged at 800 x g for 1 min. Flowthrough was discarded and the collection tube was replaced with a clean wash tube supplied in the kit. Next, 500 µL of wash buffer was added and the cartridge was centrifuged at 17 000 x g for 1 min. This step was repeated two more times, in a total of 3 wash steps and a last centrifugation was performed at 17 000 x g for 1 min to remove any residual wash buffer with ethanol.

Next, the spin cartridge was placed into a clean 1.5 mL RNA recovery tube, supplied with the kit. 50 µL of RNase-free water, heated to 65ºC was added to the cartridge and incubated for 1 min. Next, the cartridge was centrifuged at 17 000 x g for 1 min and total RNA was recovered to the tube and placed on ice and stored at -80° until further use.

RNA was then quantified NanoDrop™ spectrophotometer (Thermo Fisher Scientific).

- DNase digestion

The downstream application of the previously isolated RNA required DNA-free total RNA, therefore, a DNase I digestion was performed. All reagents were provided with the PureLink FFPE Total RNA Isolation Kit (Invitrogen). At this point, RNA concentration was normalized in all samples to 167 ng/µL. This normalization would allow, later on, a cDNA synthesis with a starting amount of 1000 ng of RNA.

For each sample, between 5-8 µL of the purified RNA was added to 1 µL of DNase I, Amplification Grade (1 U/µl), 1 µL of 10X DNase I Buffer and DEPC-treated water was added to a final volume of 10 µL. Samples were briefly vortexed and incubated at room temperature for 10 min. Samples were centrifuged briefly and 1 µL of EDTA 25 mM was added to each tube, on ice. After this, samples were incubated at 65°C for 10 min and briefly centrifuged. RNA samples were stored at -80°C until further use.

3.4.3 cDNA synthesis

To convert RNA extracts to cDNA, it was used the NZY First Strand cDNA Synthesis Kit, separate oligos (NZYTech). 6 µL of RNA of each sample were placed in a sterile, nuclease-free microcentrifuge tube and 1 µL of random hexamer mix (50 ng/µL) as well as 1 µL of 10x Annealing Buffer were added. The solution was gently mixed and incubated at 65°C for 5 mins and then placed on ice for 1 min. 10 µL of NZYRT 2x Master Mix, no oligos and 2 µL of NZYRT Enzyme Mix was then added, in order to perform the reverse-transcription step. After gently mixing the samples, these were submitted to a defined program in the BioRad T100™ Thermal Cycler: 10 min on 25ºC, 30 min on 50ºC, and 5 min at 85ºC. Lastly, 1µL of NZY RNase H was added and the samples were incubated at 37ºC for 20 mins.

3.4.4 qRT-PCR analysis

Prior to qRT-PCR analysis of sarcoma samples, a primer optimization protocol was applied due to the fact that some of the primers were recently acquired and hadn't been tested yet. Firstly, a qRT-PCR was performed with one sample in order to assess whether the primers were amplifying the specific region of interest or multiple regions. The primers tested included *ALDOC, ENO1, GAPDH, HK2, PGK1, GDH* and *MDH2*. Triplicates were performed, meaning 3 identical wells were prepared. It was concluded that the primers *ENO1, GDH* and *HK2* were not specific and therefore not used in the experiments. After this, different dilutions of the cDNA obtained were tested (1, 1:2, 1:3). It was established that a 1:3 dilution of the cDNA obtained from cDNA synthesis was performing the best. Lastly, cDNA samples were diluted with a 1:3 dilution factor, using milliQ nuclease free water.

For qRT-PCR analysis, a MicroAmp™ Optical 384-Well Reaction Plate (Applied Biosystems™) was used as well as NZYSpeedy qPCR Green Master Mix (2x), ROX (NZYTech). In each well 2 µl of cDNA was used, as well as 10 µl of NZYSpeedy qPCR Green Master Mix, 0,8 µl of forward primer (400 nM) and 0,8 µl of reverse primer (400 nM). For each sample, triplicates were performed meaning 3 identical wells were prepared. The 12k Flex & ViiA™ 7 Real-Time PCR System was programmed for: 1 cycle at 95ºC for 2 min and 40 cycles at 95ºC for 5s, followed by 15s at 65ºC. The curves obtained were evaluated based on the mean of Ct value for each gene target quantification The max ct value used for analysis of results and statistical tests was 35. The following primers were used:

Table 1- Data regarding genes used for qRT-PCR analysis

Metabolic Pathway	Gene name	Primer	Sequence
Glycolysis	*LDHA*	hLDHA-F	ACCCAGTTTCCACCATGATT
		hLDHA-R	CCCAAAATGCAAGGAACACT
	ALDOC	hALDOC-F	TCCAGGATAAGGGCATCGTC
		hALDOC-R	CCATCAGTCCCAGCTAGAGG
	GAPDH	hGAPDH-F	CAAATTCCATGGCACCGTCA
		hGAPDH-R	ATCGCCCCACTTGATTTTGG
	PGK1	hPGK1-F	GTGCCCATGCC TGACAAGTAC
		hPGK1-R	TGGGCCTACACAGTCCTTCAAG
Mitochondrial metabolism	*MDH2*	hMDH2-F	CCTGTTCAACACCAATGCCA
		hMDH2-R	GGATTGGCAATGACGCAGAT
Glutamine pathway	*GLS2*	hGLS2-F	GCCTGGGTGATTTGCTCTTTT
		hGLS2-R	CCTTTAGTGCAGTGGTGAACTT
Housekeeping gene	*18S*	h18S-F	CCCCGTTCTCTGGGAACTC
		h18S-R	TGTATGAGACCACTCTTTCCCATA

4. Results

The creation of the sarcoma sample collection at the iMM-biobank required the contribution of multiple parties. The circuit created to obtain, process and store human sarcoma samples surgically collected from patients at CHULN-HSM required several multidisciplinary meetings which included clinicians, researchers, pathologists and biobank staff, in order to optimize the circuit comprising collection of blood and tissue samples, transport of these samples to the iMM-biobank and pathology analysis, respectively, and consequent processing, classification and storage.

The 11 samples obtained correspond to the total amount of patients operated at HSM during the time period of October 2021 to September 2022. Given the rarity of this type of cancer, a reduced number of samples was obtained. Moreover, no osteosarcomas samples were collected during this period of time due to lack of equipment and protocol optimization.

Regarding processing of blood samples, from each sample were obtained: 6 aliquots of 250 uL of serum, 2 aliquots of approximately $4{,}25x10^6$ cells and one DNA pellet equivalent to $1x10^6$ cells.

Table 2- Data regarding samples collected between October 2021- September 2022

Surgery date	Sample ID	Sarcoma type	Blood Collection	Tissue collected
09/11/2021	1516018 (151)	Atypical lipomatous tumor	Yes	Normal tissue
				Tumoral tissue
07/12/2021	2856711 (285)	Undifferentiated pleomorphic sarcoma	Yes	Normal tissue
				Tumoral tissue
04/01/2022	193932 (193)	Non specified sarcoma	Yes	No tissue collected
13/01/2022	2831692 (283)	Chondrosarcoma	Yes	No tissue collected
14/01/2022	2791806 (279)	Myxoid liposarcoma metastasis	Yes	Normal tissue
				Tumoral tissue
01/02/2022	2803696 (280)	Adamantinoma	Yes	Normal tissue
				Tumoral tissue
08/03/2022	2840192 (284)	Osteosarcoma	Yes	No tissue collected
02/08/2022	451822 (451)	Leiomyosarcoma metastasis	Yes	Tumor tissue
02/08/2022	2314607 (231)	Undifferentiated pleomorphic sarcoma	Yes	Normal tissue
				Tumoral tissue
03/08/2022	1865228 (186)	Dermatofibrosarcoma protuberans	Yes	Normal tissue
				Tumoral tissue

03/08/2022	610528 (610)	Leiomyosarcoma	Yes	Normal tissue
				Tumoral tissue

4.1 NMR evaluation

Regarding NRM evaluation, 6 of the 11 samples were analyzed to date: 186, 231, 279, 280, 285, 610. Figure 3 represents a TOCSY (Total Correlation Spectroscopy) spectrum and figure 4 represents expansions of 500 MHz 1H NMR spectra of the 280 sample pair. The former is a 2D experiment that creates correlations between all protons within a given spin system[42] and was obtained in order to correctly attribute metabolite signals present in the 1D spectra.

Among the analyzed samples, the pairs 280 and 285 revealed consistent data, as shown in figure 4. These preliminary results on 1H NMR profiling of STS display evident differences between tumoral tissue and adjacent non-involved healthy tissue. Tumor samples indicate high glycolytic activity by displaying higher levels of lactate alongside lower levels of glucose. Furthermore, increased levels of glutamate are shown together with lower levels of glutamine, which suggests a higher glutamine metabolism in these samples. Altered levels of glucose-1-phosphate and UDP-glucose also imply alterations in glycogen metabolism. Lastly, differences comprising increased levels of branched chain and aromatic amino acids, as well as acetate and decreased levels of carnosine, glycerophosphocholine and creatine are noticeable.

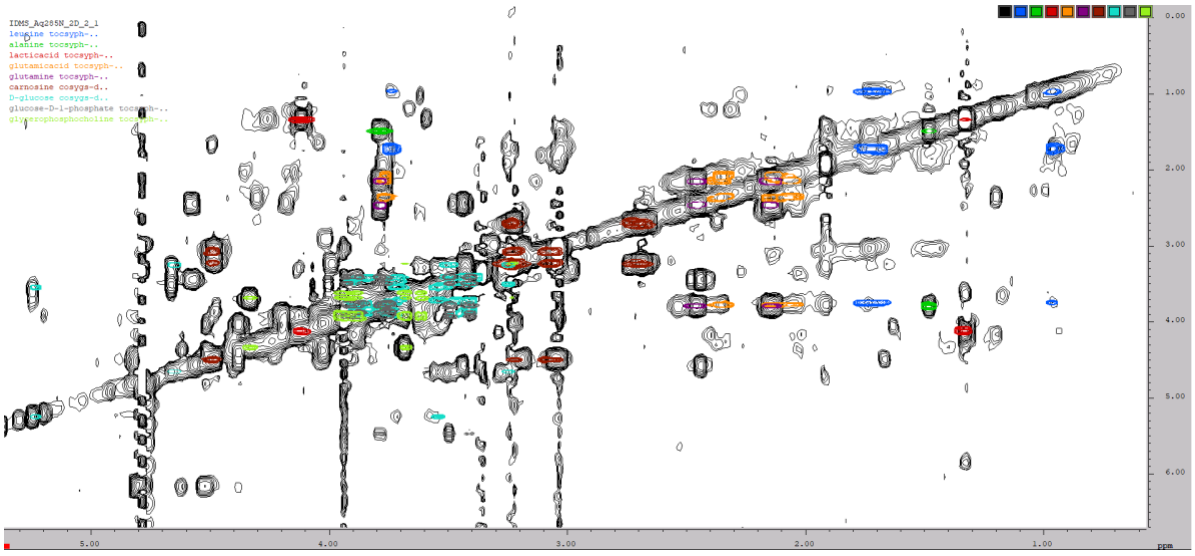

Fig. 3- TOCSY spectra of a representative sample

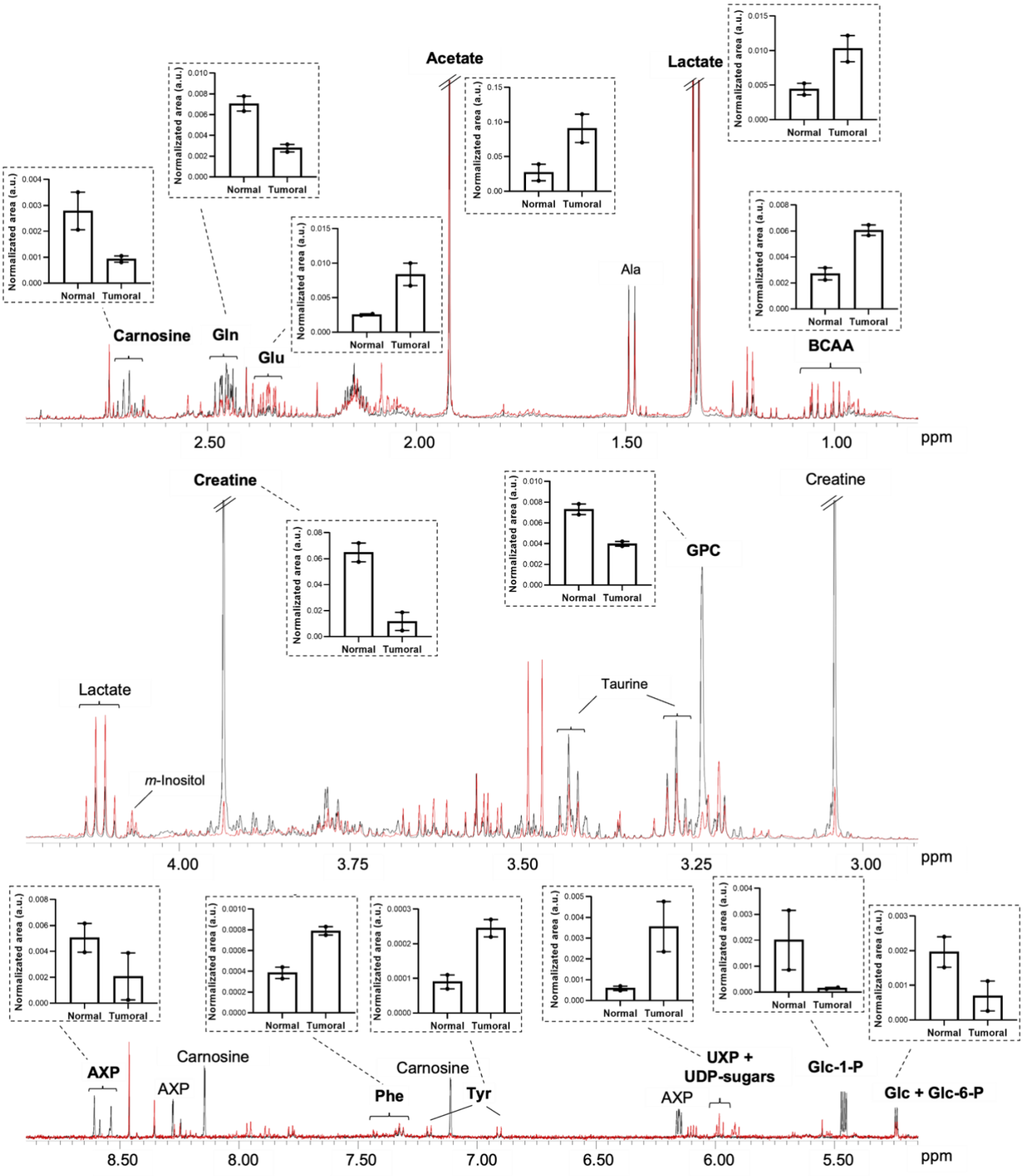

Fig. 4- Expansions of 500 MHz 1H NMR spectra of a representative pair of tissue extracts from sarcoma (in red) and adjacent non-involved normal tissue (in black). The relative abundances of selected metabolites displaying consistent differences between two tissue pairs are shown graphically. The error bars represent the mean with range. No statistics were applied due to the small number of samples per group.

Further analysis of more samples allowed to assess the consistence of the differences displayed before. Figure 5 represents a heatmap concerning all 6 samples analyzed. It shows a clear separation of metabolites highly present in tumor samples vs healthy tissue samples. The more accentuated differences concern carnosine, glycerophosphochol, creatine, glucose+glucose-6-phosphate and glucose-1-phosphate, displaying higher levels in normal samples and amino acids tyrosine, isoleucine, leucine, alanine as well as lactate, glutamate and UXP+UPD-sugars displaying higher levels on tumor samples.

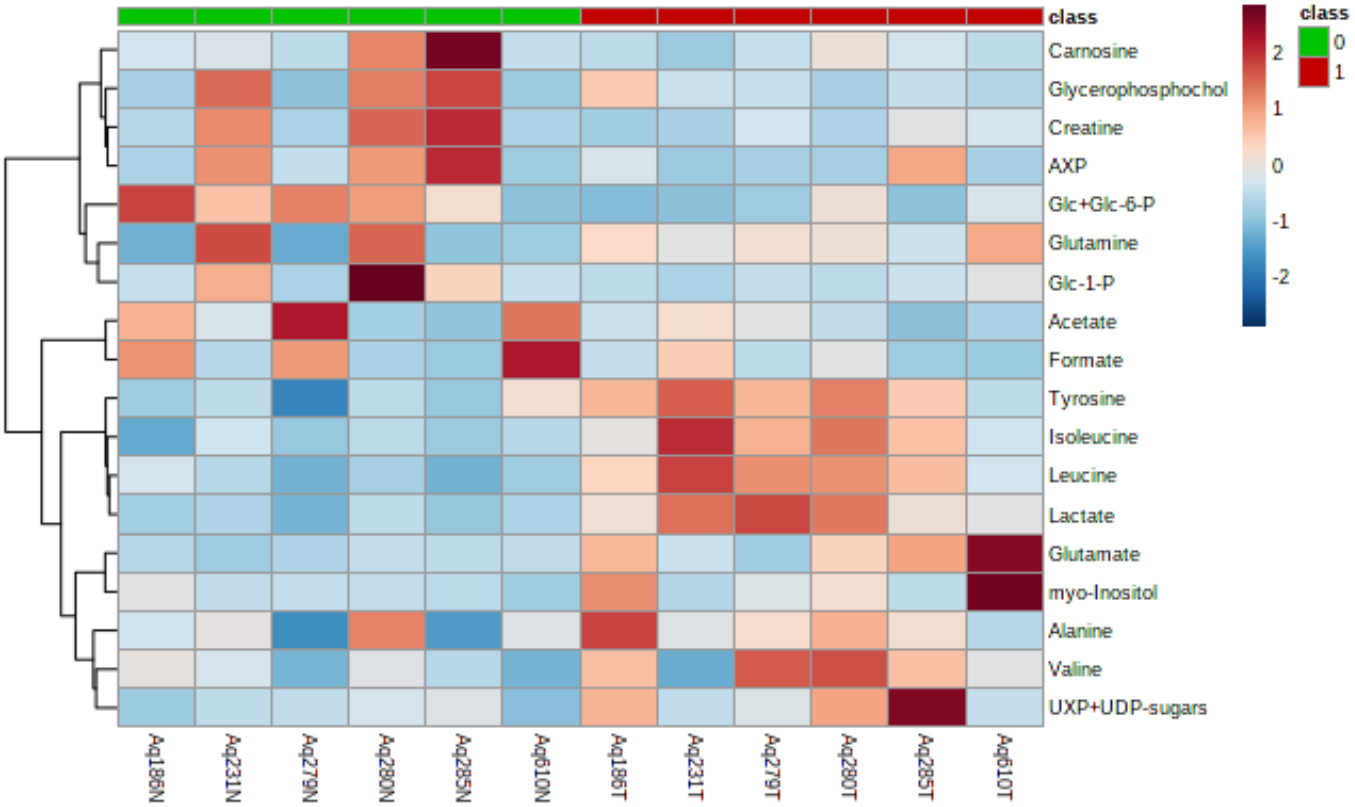

Fig. 5- Heatmap- Spectral Integration of the 6 analyzed pairs. 18 signal areas were measured (representative of known metabolites, without significant overlap)

The same differences can be seen in the graphical representation of fold change (FC) (fig. 6 and 7). Regarding higher levels in tumors, the most prominent differences concern metabolites such as leucine, isoleucine and lactate. Concerning lower levels in tumors, glucose, creatine and AXP standout.

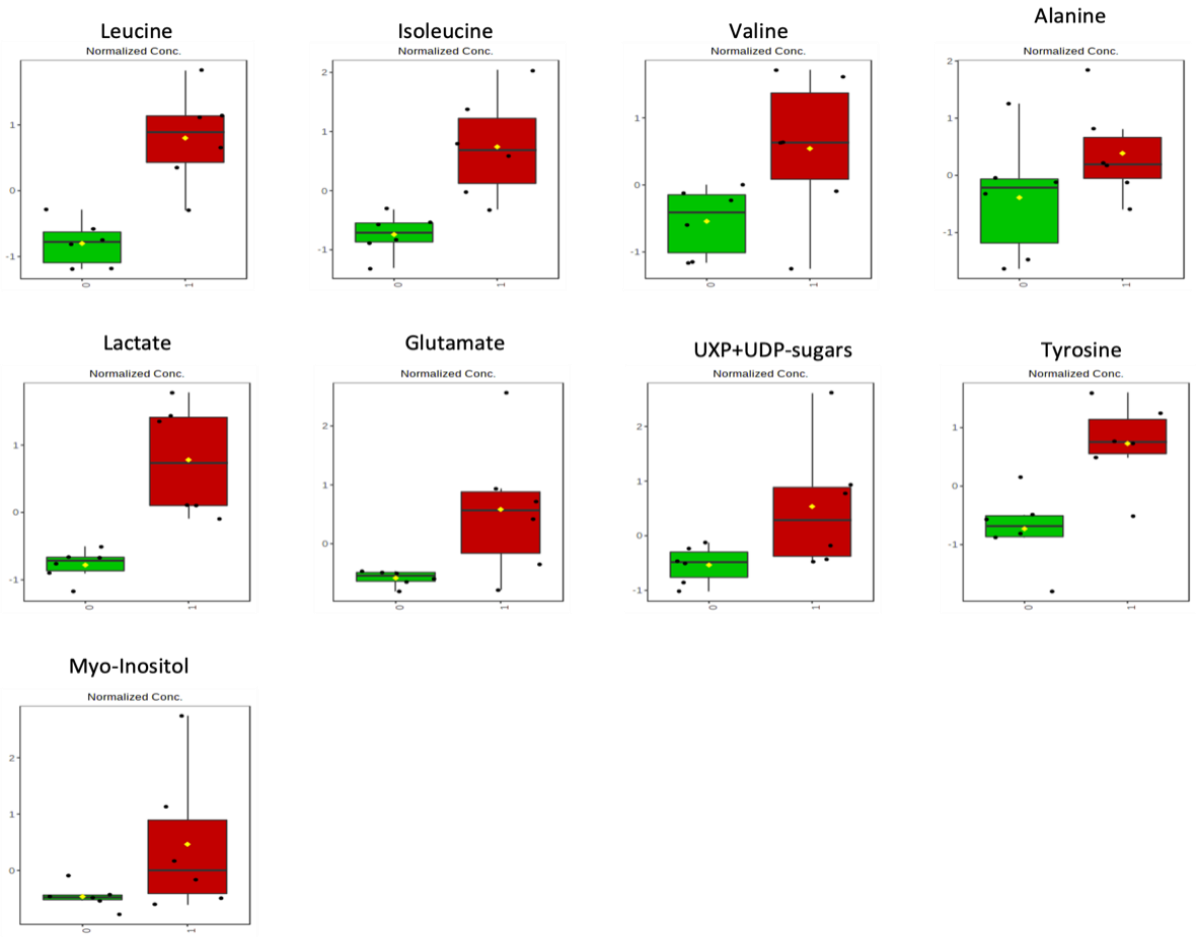

Fig. 6- Graphical representation of metabolites with higher levels in tumors (red). Spectral Integration of the 6 analyzed pairs. 18 signal areas were measured (representative of known metabolites, without significant overlap)

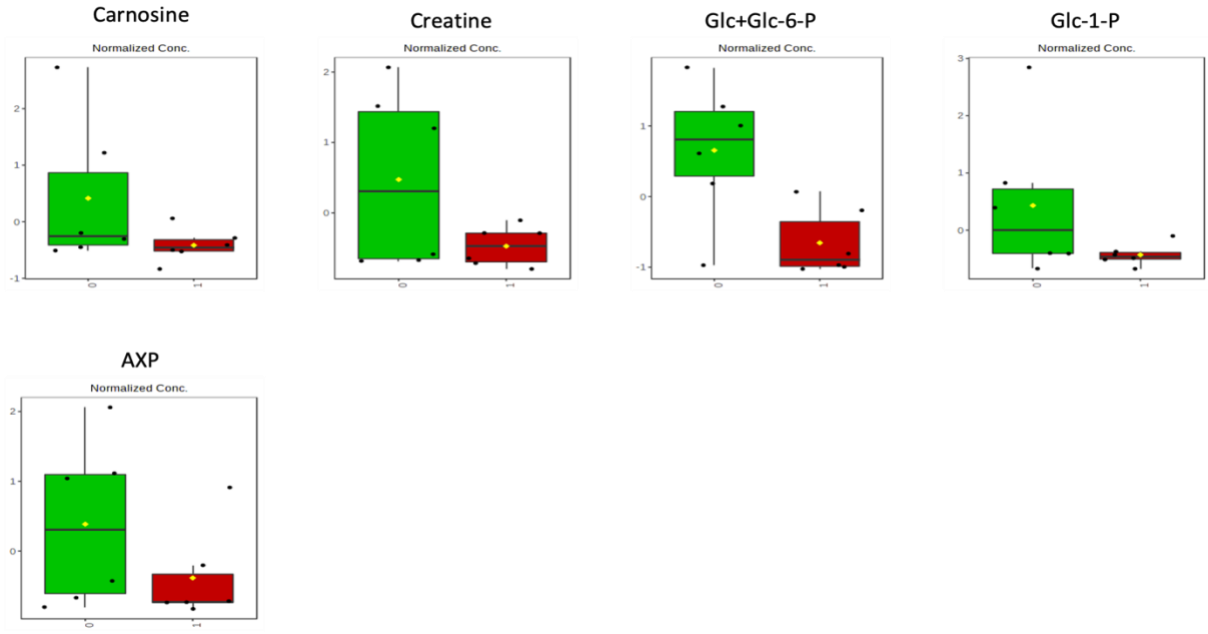

Fig. 7- Graphical representation of metabolites with lower levels in tumors (red). Spectral Integration of the 6 analyzed pairs. 18 signal areas were measured (representative of known metabolites, without significant overlap)

4.2 qRT-PCR

Regarding expression of genes involved in glycolysis, the preliminary results obtained show a higher expression of *LDHA,* followed by *GAPDH* and *ALDOC*. Evaluating by the expression of MDH2, mitochondrial metabolism seems active as well. *GLS2*, involved in glutamine metabolism, shows the lowest level of expression amongst the assessed genes.

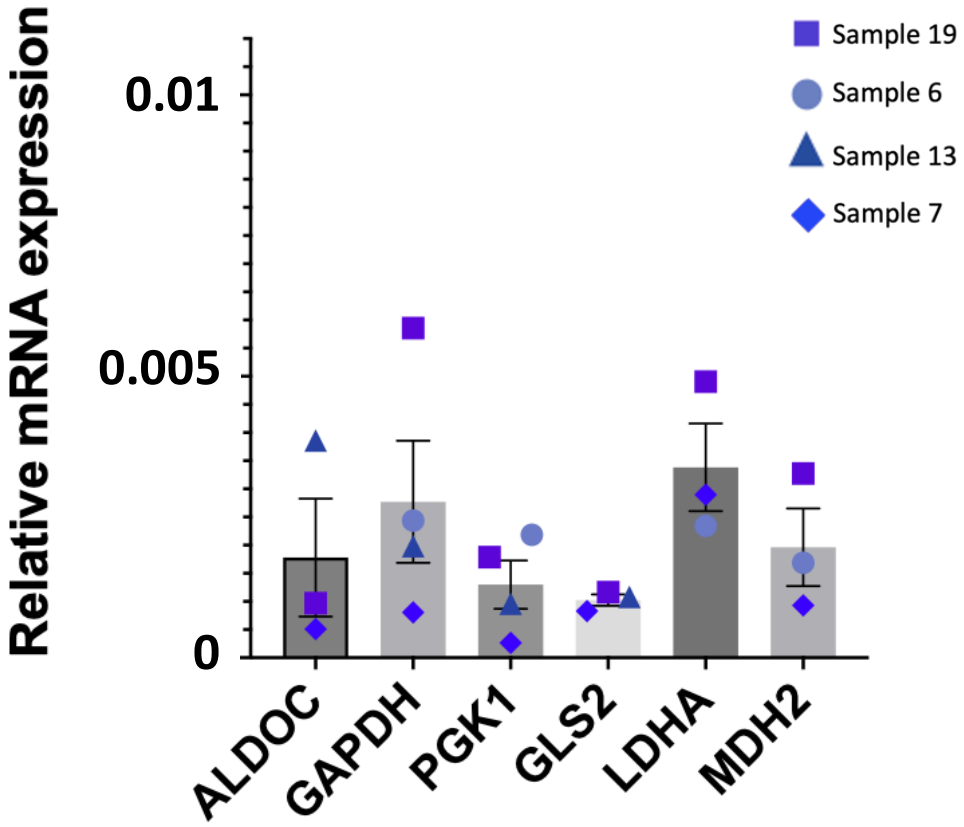

Fig. 8- Relative mRNA expression of genes involved in glycolysis (ALDOC, GAPDH, PGK1, LDHA), in glutamine metabolism (GLS2) and in mitochondrial metabolism (MDH2). Data are presented as mean ±SEM.

5. Discussion

There is an urge to improve knowledge on sarcomagenesis and the mechanisms underlying disease onset and progression. Therefore the goal of starting to assess sarcoma metabolic profile by applying NMR analysis was not solely the identification of all metabolites present in each sample, but rather the identification and quantification of features that might vary significantly between two groups of samples: tumor tissue vs adjacent normal tissue. According to the results we obtained, it was possible to assess that STS cells exhibited high glycolytic activity by displaying high levels of lactate alongside lower levels of glucose. This has been shown before, by Sharma et al. who compared differences between tumor and normal tissue using STS from 19 patients, performing 2D NMR experiments[50]. The authors observed that tumor tissue displayed a higher concentration of lactate as well as an elevated concentration of glycerophosphocholine and choline (membrane metabolites).

Di Gialleonardo et al. assessed the *in vitro* effect of inhibiting the PI3K/mTOR pathway in cell lines using ^{1}H NMR spectroscopy as well as hyperpolarized [1-^{13}C] pyruvate magnetic resonance to evaluate the *in vivo* effects of that same inhibition[51]. The latter prompted an overall decrease in lactate production *in vitro* followed by cell growth inhibition. Regarding *in vivo* assessment, a similar effect was observed, with a reduction in lactate production alongside changes in tumor size. This study highlighted the importance of ^{1}H NMR spectroscopy and hyperpolarized [1-^{13}C] pyruvate magnetic resonance spectroscopy in the assessment of effects induced by pharmacological inhibition of the PI3K/mTOR pathway[51].

Regarding glutamine metabolism, our results showed increased levels of glutamate together with lower levels of glutamine, indicating a higher glutamine metabolism in these samples. In fact, Lee et al. demonstrated the critical dependency of tumor cells from a UPS mouse model on glutaminolysis, using a combination of LC-MS and stable isotope metabolite tracing[22]. The authors showed that murine UPS and human fibrosarcoma and leiomyosarcoma cell proliferation is dependent on glutamate derived from glutamine, in contradiction of what was observed for healthy muscle cells. This metabolism was supporting central carbon metabolism, aspartate production, nucleotide biosynthesis and consequently, cell proliferation. The authors also concluded this dependency was largely due to defective anaplerosis upon glutamine deprivation. Taking into consideration the significant dependency of UPS on glutamine, the authors tested the therapeutic effects of telaglenastat (CB-839), which is a GLS inhibitor, *in vivo* and *in vitro*, and showed promising results, with CB-839 blocking GLS activity and UPS tumor growth both *in vitro* and *in vivo*. The use of GLS inhibitors is now under clinical trials in humans[33]. Data obtained from our NMR analysis is in concordance with the latter. However, our qPCR results show a lower *GLS2* expression when compared to glycolytic genes. This divergence might be due to the poor quality of the RNA extracted and analyzed or might indeed translate that the samples evaluated when relying more on glycolysis than glutamine metabolism. Another technical approach was used by Lemberg et al. to obtain information on the metabolomics of sarcomas, showing a high dependence of malignant peripheral nerve sheath tumors (MPNST) on glutamine[52]. They

observed that MPNST cells required elevated concentrations of this metabolite in order to restart their proliferation after glutamine starvation. The authors tested a glutamine antagonist, JHU395, discovering a significant inhibition of MPNST growth *in vivo* and, using mass spectrometry, evaluated 400 metabolites from samples of MPNST previously treated with JHU935. The results obtained showed a statistically significant fold change between vehicle and JHU395-treated tumors for 18 metabolites. Formylglycinamide ribonucleotide presented as the most altered metabolite between the two conditions.

Interestingly, in a study investigating the effects of arginine auxotrophy, induced by ASS1 deficiency, on the progression of tumors, the authors used a pegylated arginine deiminase (ADI-PEG20) in order to deplete arginine[53]. This treatment, when applied to LMS cell lines, immediately induced cell proliferation arrest. However, when treatment was extended over a larger period of time, cell lines became resistant to ADI-PEG20 due to the reexpression of ASS1 and consequent regeneration of arginine. A metabolomic profiling study of these treated cell lines showed an overall reduction in PKM2 levels, while $U^{13}C$ glucose tracing studies revealed that carbons were shifted away from lactate and citrate production and reoriented toward serine/glycine synthesis[33,53]. These cells were actually exhibiting a reduced reliance on glucose and reinforcing OXPHOS and glutaminolysis as an alternative source of TCA cycle intermediates via anaplerosis. Currently, there is an ongoing trial, combining ADI-PEG20 with Gemcitabine and Docetaxel to treat STS[33].

Regarding current knowledge on STS, there is a significant heterogeneity within each subtype and between different subtypes, as it is also possible to assess through the variation of some metabolites in our results (fig. 7). This elevated variation, seen mostly in healthy samples, might also be due to the fact that the spectra obtained from these samples was noisier when compared to the tumor pairs. This can be due to a poorer extraction of metabolites from these samples either at the maceration or extraction steps. When only considering the 3 most consistent pairs analyzed (231, 280, 285) the variations between samples for the same metabolite are much lower (see annex figure 1). Analysis of higher sample numbers is underway in order to verify the continuous consistence of these differences and assess their discriminative power between STS and healthy tissue.

The aerobic glycolytic profile and level of OXPHOS vary with different tumors and the balance between these two may be influenced by numerous metabolic oncogenic adaptations[33,54]. One interesting example of crosstalk between metabolic pathways in cancer lies on the expression of various phosphofructokinase (PFK) isoenzymes by cancer cells as an adaptation to overcome ATP-dependent inhibition of PFK-1[33]. The latter catalyzes the upstream reaction committing glucose to glycolysis and is allosterically inhibited by high ATP levels in normal conditions. Therefore, by expressing PFK enzymes such as the bifunctional 6-phosphofructo-2-kinase/ fructose-2,6-bisphosphatase (PFKFB) that produces F2,6-BP, these cells override PFK1 inhibition[33]. However, an activation of a F1,6-biphosphatase like FBP1 augments the gluconeogenic flow and restrains glycolysis[33,55]. The FBP2 isoform is often lost in STS including LPS, FS, LMS and UPS [56,57]. One study showed that enhancing FBP2 expression

impairs sarcoma cell growth by inhibiting glycolysis and promoting mitochondrial biogenesis[56].

Tumor metabolome is a clear influence on STS progression and the metabolomic and multi-omics studies on STS mentioned before have already allowed the identification of various cancer cell metabolic characteristics, which lead to the elaboration of alternative approaches targeting glucose and glutamine metabolism, as well as fatty acid metabolism, highlighting the importance of metabolome assessment by metabolomic approaches.

For qRT-PCR studies, FFPE sarcoma samples were used. Due to the instability of human samples, the waiting time between collection of the sample, transport and processing by the pathologist and also the type of storage (FFPE) are all processes that speed up the degradation rate of these samples. Therefore, the RNA extracted from these samples was highly degraded as well as contaminated. From the preliminary results that were possible to acquire, a higher expression of LDHA is noticeable, which was expected, given the high concentrations of lactate assessed by NMR.

Hanwen Chen et al. showed that miR-323a-3p was significantly downregulated in osteosarcoma (OS) tissues and cell lines and that an overexpression of miR-323a-3p caused a decrease in cell viability and induction of apoptosis[58]. Through bioinformatic analysis, the authors predicted *LDHA* to be a target of miR-323a-3p. In fact, a high expression of miR-323a-3p significantly reduced mRNA and protein levels of LDHA, attenuating lactate production. Ultimately the authors show that miR-323a-3p suppressed the growth of OS cells by targeting LDHA and inhibiting glycolysis of OS.

Moreover, Mengkai Yang et al. examined 198 glycolysis-related genes with the goal of identifying a gene signature for the prediction of the prognosis of OS patients[59]. In this study they identified 3 genes (*P4HA1, ABCB6* and *STC2*) for the establishment of a risk signature. Based on the signature, patients included in the high-risk group had poor outcomes. In this study they show that key genes of the glycolytic pathway such as *HK2, ENO1* and *LDHA* displayed elevated levels of expression in the high-risk group.

Shuang Zhang et al. aimed to identify protein markers implicated in resistance to chemotherapy drugs, such as cisplatin, in osteosarcoma patients[60]. They found five significantly expressed proteins including PGK1, that may be an appropriate marker used upon treatment with cisplatin.

Although it is not possible to state much about glycolytic gene alterations in sarcomagenesis from our preliminary results, it is of high importance to continue this approach regarding one of the main metabolic pathways involved in cancer progression. A bigger number of samples as well as a wider panel of genes involved in glycolysis, glutamine metabolism and mitochondrial activity will enlighten the likely important mechanisms underlying the development of STS.

Currently, and to our knowledge, there is no evidence of a sarcoma biobank collection created elsewhere. Given the rarity of this type of cancer, the creation of a collection of Sarcoma samples for future studies holds great value.

6. General conclusion

Current treatment options for STS patients are based on a “fit for all” principle, despite the metabolic and genetic differences between STS subtypes. Moreover, the long-term success rate is dismal, with 40% of patients diagnosed with sarcoma dying due to disease progression[32]. Therefore, there is an urge to improve diagnosis as well as create new hypothesis on sarcomagenesis mechanisms and investigate new approaches. The work presented here enlightens a very small part of the mechanisms underlying STS. It was shown that different sarcoma subtypes have common metabolic characteristics such as elevated glycolysis and glutamine metabolism, which is in concordance with data previously described by other authors. Furthermore, there was a clear separation of predominant metabolites in the two different groups analyzed (tumor tissue vs normal tissue). However, analysis of a higher sample number is crucial for the establishment of discriminative differences between STS and healthy tissue.

Lastly, the creation of a sarcoma sample collection has the potential to contribute to numerous studies and different approaches that will consequently, add valuable knowledge to this area.

7. Future perspectives

The work presented on this Thesis represents part of a bigger project regarding the characterization of Sarcomas. Alongside this work there is an ongoing project, taking place in the USA, concerning gene expression and transcriptomics of STS human samples. Furthermore, it would be of great value to assess gene expression on the same sarcoma samples used for NMR analysis. Additionally, assessment of protein expression in these same samples can be beneficial given the fact that, altogether, this would allow a more complete assessment of the metabolic profile of STS.

References

1. Sudhakar, A. History of Cancer, Ancient and Modern Treatment Methods. *J. Cancer Sci. Ther.* **1**, 1–4 (2009).
2. Bray, F. *et al.* Global cancer statistics 2018: GLOBOCAN estimates of incidence and mortality worldwide for 36 cancers in 185 countries. *CA. Cancer J. Clin.* **68**, 394–424 (2018).
3. Hanahan, D. & Weinberg, R. A. The hallmarks of cancer. *Cell* **100**, 57–70 (2000).
4. Loeb, K. R. & Loeb, L. A. Significance of multiple mutations in cancer. *Carcinogenesis* **21**, 379–385 (2000).
5. Hanahan, D. & Weinberg, R. A. Hallmarks of cancer: the next generation. *Cell* **144**, 646–674 (2011).
6. Hanahan, D. Hallmarks of Cancer: New Dimensions. *Cancer Discov.* **12**, 31–46 (2022).
7. Vanneman, M. & Dranoff, G. Combining immunotherapy and targeted therapies in cancer treatment. *Nat. Rev. Cancer* **12**, 237–251 (2012).
8. Gerber, D. E. Targeted therapies: A new generation of cancer treatments. *Am. Fam. Physician* **77**, 311–319 (2008).
9. Zheng, H.-C. The molecular mechanisms of chemoresistance in cancers. *Oncotarget* **8**, 59950–59964 (2017).
10. Pavlova, N. N. & Thompson, C. B. The Emerging Hallmarks of Cancer Metabolism. *Cell Metab.* **23**, 27–47 (2016).
11. DeBerardinis, R. J. & Chandel, N. S. Fundamentals of cancer metabolism. *Sci. Adv.* **2**, e1600200 (2016).
12. Vander Heiden, M. G. & DeBerardinis, R. J. Understanding the Intersections between Metabolism and Cancer Biology. *Cell* **168**, 657–669 (2017).
13. Koppenol, W. H., Bounds, P. L. & Dang, C. V. Otto Warburg's contributions to current concepts of cancer metabolism. *Nat. Rev. Cancer* **11**, 325–337 (2011).
14. Mendes, C. & Serpa, J. Metabolic Remodelling: An Accomplice for New Therapeutic Strategies to Fight Lung Cancer. *Antioxidants (Basel, Switzerland)* **8**, (2019).
15. Adekola, K., Rosen, S. T. & Shanmugam, M. Glucose transporters in cancer metabolism. *Curr. Opin. Oncol.* **24**, 650–654 (2012).
16. Serpa, J. *Metabolic Remodeling as a Way of Adapting to Tumor Microenvironment (TME), a Job of Several Holders*. (2020).
17. Szablewski, L. Expression of glucose transporters in cancers. *Biochim. Biophys. Acta* **1835**, 164–169 (2013).
18. Ishikawa, N., Oguri, T., Isobe, T., Fujitaka, K. & Kohno, N. SGLT gene expression in primary lung cancers and their metastatic lesions. *Jpn. J. Cancer Res.* **92**, 874–879 (2001).
19. Rempel, A., Mathupala, S. P., Griffin, C. A., Hawkins, A. L. & Pedersen, P. L. Glucose catabolism in cancer cells: amplification of the gene encoding type II hexokinase. *Cancer Res.* **56**, 2468–2471 (1996).
20. Hay, N. Reprogramming glucose metabolism in cancer: can it be exploited for cancer therapy? *Nat. Rev. Cancer* **16**, 635–649 (2016).
21. Martinez-Outschoorn, U. E., Peiris-Pagés, M., Pestell, R. G., Sotgia, F. & Lisanti, M. P. Cancer metabolism: a therapeutic perspective. *Nat. Rev. Clin. Oncol.* **14**, 11–31 (2017).
22. Lee, P. *et al.* Targeting glutamine metabolism slows soft tissue sarcoma growth. *Nat. Commun.* **11**, (2020).
23. Esperança-martins, M. *et al.* Sarcoma Metabolomics : Current Horizons and Future

Perspectives. (2021).
24. Issaq, S. H., Mendoza, A., Fox, S. D. & Helman, L. J. Glutamine synthetase is necessary for sarcoma adaptation to glutamine deprivation and tumor growth. *Oncogenesis* **8**, (2019).
25. Esperança-Martins, M. *et al.* Sarcoma metabolomics: Current horizons and future perspectives. *Cells* **10**, (2021).
26. Wallace, D. C. Mitochondria and cancer. *Nat. Rev. Cancer* **12**, 685–698 (2012).
27. Guerra, F., Arbini, A. A. & Moro, L. Mitochondria and cancer chemoresistance. *Biochim. Biophys. Acta - Bioenerg.* **1858**, 686–699 (2017).
28. Hsu, C. C., Tseng, L. M. & Lee, H. C. Role of mitochondrial dysfunction in cancer progression. *Exp. Biol. Med.* **241**, 1281–1295 (2016).
29. Phan, L. M., Yeung, S. C. J. & Lee, M. H. Cancer metabolic reprogramming: importance, main features, and potentials for precise targeted anti-cancer therapies. *Cancer Biol. Med.* **11**, 1–19 (2014).
30. Chang, L., Fang, S. & Gu, W. The Molecular Mechanism of Metabolic Remodeling in Lung Cancer. *J. Cancer* **11**, 1403–1411 (2020).
31. Miallot, R., Galland, F., Millet, V., Blay, J. Y. & Naquet, P. Metabolic landscapes in sarcomas. *J. Hematol. Oncol.* 1–23 (2021) doi:10.1186/s13045-021-01125-y.
32. Nacev, B. A. *et al.* Clinical sequencing of soft tissue and bone sarcomas delineates diverse genomic landscapes and potential therapeutic targets. *Nat. Commun.* **13**, 3405 (2022).
33. Miallot, R., Galland, F., Millet, V., Blay, J. Y. & Naquet, P. Metabolic landscapes in sarcomas. *J. Hematol. Oncol.* **14**, 1–23 (2021).
34. Comprehensive and Integrated Genomic Characterization of Adult Soft Tissue Sarcomas. *Cell* **171**, 950-965.e28 (2017).
35. Xu, D. *et al.* The Evolving Landscape of Noncanonical Functions of Metabolic Enzymes in Cancer and Other Pathologies. *Cell Metab.* **33**, 33–50 (2021).
36. Goncalves, M. D., Hopkins, B. D. & Cantley, L. C. Phosphatidylinositol 3-Kinase, Growth Disorders, and Cancer. *N. Engl. J. Med.* **379**, 2052–2062 (2018).
37. Li, X. *et al.* Mitochondria-Translocated PGK1 Functions as a Protein Kinase to Coordinate Glycolysis and the TCA Cycle in Tumorigenesis. *Mol. Cell* **61**, 705–719 (2016).
38. Zhang, B. *et al.* Arginine methyltransferase inhibitor-1 inhibits sarcoma viability in vitro and in vivo. *Oncol. Lett.* **16**, 2161–2166 (2018).
39. Hollywood, K., Brison, D. R. & Goodacre, R. Metabolomics: current technologies and future trends. *Proteomics* **6**, 4716–4723 (2006).
40. Bingol, K. Recent Advances in Targeted and Untargeted Metabolomics by NMR and MS / NMR Methods. (2018) doi:10.3390/ht7020009.
41. Min, L., Choy, E., Tu, C. & Hornicek, F. Application of metabolomics in sarcoma: From biomarkers to therapeutic targets. *Crit. Rev. Oncol. Hematol.* **116**, (2017).
42. Gowda, G. A. N. & Raftery, D. NMR Based Metabolomics. 19–37 (2022) doi:10.1007/978-3-030-51652-9.
43. Trezzi, J.-P., Vlassis, N. & Hiller, K. The Role of Metabolomics in the Study of Cancer Biomarkers and in the Development of Diagnostic Tools. *Adv. Exp. Med. Biol.* **867**, 41–57 (2015).
44. Mercier, K. A., Al-jazrawe, M., Poon, R., Acu, Z. & Alman, B. OPEN A Metabolomics Pilot Study on Desmoid Tumors and Novel Drug Candidates. 1–12 (2018)

doi:10.1038/s41598-017-18921-7.
45. Wang, S., Blair, I. A. & Mesaros, C. Analytical Methods for Mass Spectrometry-Based Metabolomics Studies. (2019) doi:10.1007/978-3-030-15950-4.
46. Kelly, A. D. *et al.* Metabolomic Profiling from Formalin-Fixed , Paraffin- Embedded Tumor Tissue Using Targeted LC / MS / MS : Application in Sarcoma. **6**, (2011).
47. Lou, S., Balluff, B., Cleven, A. H. G., Bovée, J. V. M. G. & Mcdonnell, L. A. Prognostic Metabolite Biomarkers for Soft Tissue Sarcomas Discovered by Mass Spectrometry Imaging. 376–383 (2016) doi:10.1007/s13361-016-1544-4.
48. Kalfe, A., Telfah, A., Lambert, J. & Hergenröder, R. Looking into Living Cell Systems: Planar Waveguide Microfluidic NMR Detector for in Vitro Metabolomics of Tumor Spheroids. *Anal. Chem.* **87**, 7402–7410 (2015).
49. Patra, B., Sharma, M., Hale, W. & Utz, M. Time-resolved non-invasive metabolomic monitoring of a single cancer spheroid by microfluidic NMR. *Sci. Rep.* **11**, 53 (2021).
50. Sharma, U., Kar, M., Juyal, S., et al. Biochemistry of Soft Tissue Tumors : An in vitro NMR Study. **15**, 3682 (2007).
51. Di Gialleonardo, V. *et al.* Multinuclear NMR and MRI Reveal an Early Metabolic Response to mTOR Inhibition in Sarcoma. *Cancer Res.* **77**, 3113–3120 (2017).
52. Lemberg, K. M. *et al.* The Novel Glutamine Antagonist Prodrug JHU395 Has Antitumor Activity in Malignant Peripheral Nerve Sheath Tumor. *Mol. Cancer Ther.* **19**, 397–408 (2020).
53. Kremer, J. C. *et al.* Arginine Deprivation Inhibits the Warburg Effect and Upregulates Glutamine Anaplerosis and Serine Biosynthesis in ASS1-Deficient Cancers. *Cell Rep.* **18**, 991–1004 (2017).
54. Han, J. *et al.* Her4 promotes cancer metabolic reprogramming via the c-Myc-dependent signaling axis. *Cancer Lett.* **496**, 57–71 (2021).
55. Li, B. *et al.* Fructose-1,6-bisphosphatase opposes renal carcinoma progression. *Nature* **513**, 251–255 (2014).
56. Huangyang, P. *et al.* Fructose-1,6-Bisphosphatase 2 Inhibits Sarcoma Progression by Restraining Mitochondrial Biogenesis. *Cell Metab.* **31**, 174-188.e7 (2020).
57. Das, B., Jain, N. & Mallick, B. Ribonucleotide reductase subunit M2 is a potential prognostic marker and therapeutic target for soft tissue sarcoma. *Gene* **808**, 145988 (2022).
58. Chen, H., Gao, S. & Cheng, C. MiR-323a-3p suppressed the glycolysis of osteosarcoma via targeting LDHA. *Hum. Cell* **31**, 300–309 (2018).
59. Yang, M., Ma, X., Wang, Z., Zhang, T. & Hua, Y. Identification of a novel glycolysis-related gene signature for predicting the prognosis of osteosarcoma patients. *Aging (Albany. NY).* **13**, 12896–12918 (2021).
60. Zhang, S., Qin, Y. P., Kuang, J. M. & Liu, Y. H. Proteomic investigation of resistance to chemotherapy drugs in osteosarcoma. *Technol. Health Care* **26**, 145–153 (2018).

Anex

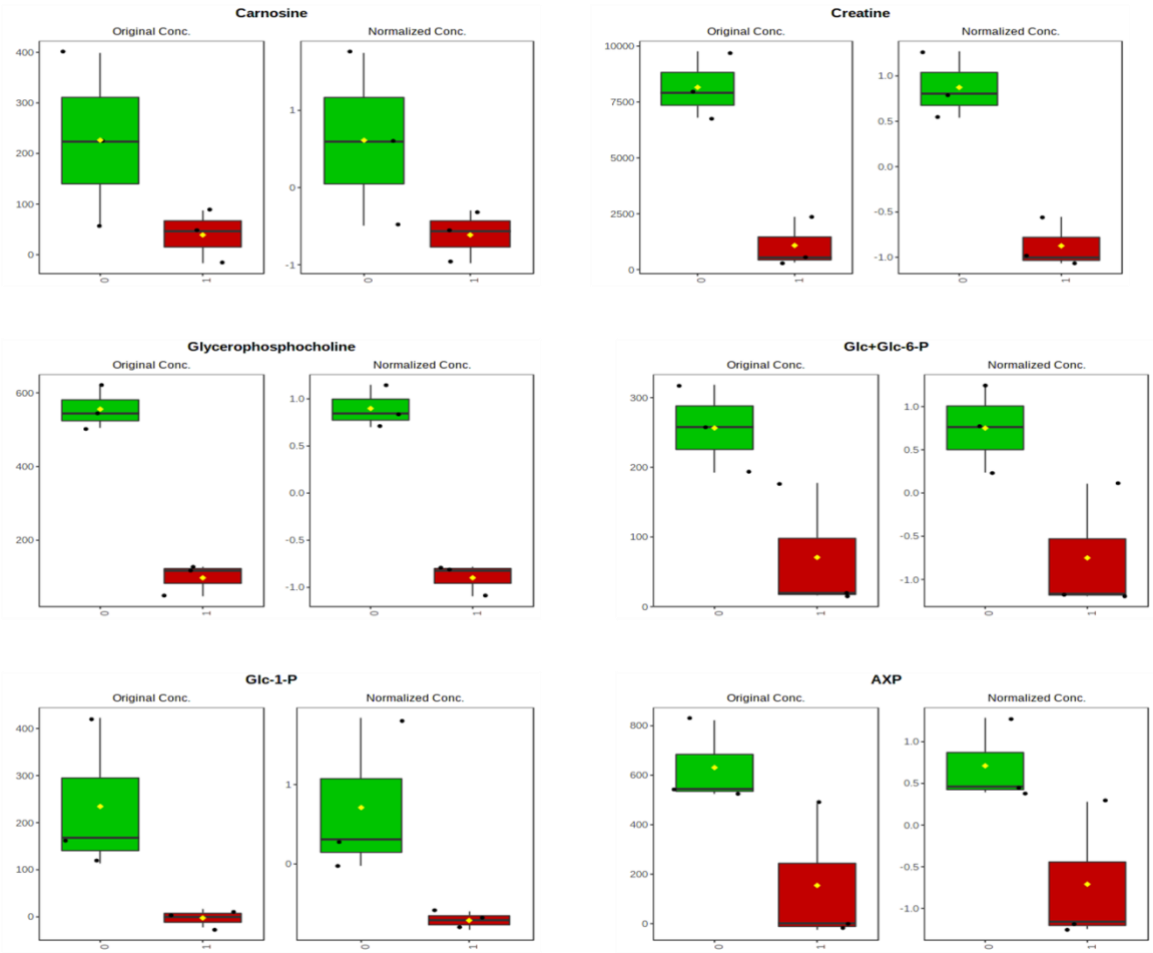

Fig. 1- Graphical representation of metabolites with lower levels in tumors (red). Spectral Integration of 3 analyzed pairs, excluding noisier spectra. 18 signal areas were measured (representative of known metabolites, without significant overlap)

International Journal of
Molecular Sciences

MDPI

Review

On the Relevance of Soft Tissue Sarcomas Metabolic Landscape Mapping

Miguel Esperança-Martins [1,2,3,*], Iola F.Duarte [4], Mara Rodrigues [2], Joaquim Soares do Brito [5], Dolores López-Presa [6], Luís Costa [1,3,7], Isabel Fernandes [1,3,7] and Sérgio Dias [2,7]

1 Medical Oncology Department, Centro Hospitalar Universitário Lisboa Norte, 1649-028 Lisboa, Portugal
2 Vascular Biology & Cancer Microenvironment Lab, Instituto de Medicina Molecular João Lobo Antunes, Faculdade de Medicina da Universidade de Lisboa, 1649-028 Lisboa, Portugal
3 Translational Oncobiology Lab, Instituto de Medicina Molecular João Lobo Antunes, Faculdade de Medicina da Universidade de Lisboa, 1649-028 Lisboa, Portugal
4 CICECO-Aveiro Institute of Materials, Department of Chemistry, Universidade de Aveiro, 3810-193 Aveiro, Portugal
5 Orthopedics Department, Centro Hospitalar Universitário Lisboa Norte, 1649-028 Lisboa, Portugal
6 Pathology Department, Centro Hospitalar Universitário Lisboa Norte, 1649-028 Lisboa, Portugal
7 Faculdade de Medicina da Universidade de Lisboa, Clínica Universitária de Oncologia Médica, 1649-028 Lisboa, Portugal
* Correspondence: miguelmemartins@campus.ul.pt

Abstract: Soft tissue sarcomas (STS) prognosis is disappointing, with current treatment strategies being based on a "fit for all" principle and not taking distinct sarcoma subtypes specificities and genetic/metabolic differences into consideration. The paucity of precision therapies in STS reflects the shortage of studies that seek to decipher the sarcomagenesis mechanisms. There is an urge to improve STS diagnosis precision, refine STS classification criteria, and increase the capability of identifying STS prognostic biomarkers. Single-omics and multi-omics studies may play a key role on decodifying sarcomagenesis. Metabolomics provides a singular insight, either as a single-omics approach or as part of a multi-omics strategy, into the metabolic adaptations that support sarcomagenesis. Although STS metabolome is scarcely characterized, untargeted and targeted metabolomics approaches employing different data acquisition methods such as mass spectrometry (MS), MS imaging, and nuclear magnetic resonance (NMR) spectroscopy provided important information, warranting further studies. New chromatographic, MS, NMR-based, and flow cytometry-based methods will offer opportunities to therapeutically target metabolic pathways and to monitorize the response to such metabolic targeting therapies. Here we provide a comprehensive review of STS omics applications, comprising a detailed analysis of studies focused on the metabolic landscape of these tumors.

Keywords: soft tissue sarcoma; single-omics; multi-omics; metabolomics; mass spectrometry; chromatography; mass spectrometry imaging; nuclear magnetic resonance

Citation: Esperança-Martins, M.; F.Duarte, I.; Rodrigues, M.; Soares do Brito, J.; López-Presa, D.; Costa, L.; Fernandes, I.; Dias, S. On the Relevance of Soft Tissue Sarcomas Metabolic Landscape Mapping. *Int. J. Mol. Sci.* **2022**, *23*, 11430. https://doi.org/10.3390/ijms231911430

Academic Editor: Walter Wahli

Received: 30 August 2022
Accepted: 23 September 2022
Published: 28 September 2022

1. Concept and Utility of Single-Omics or Multi-Omics Strategies to Identify Biomarkers and Therapeutic Targets in Sarcomas

Sarcomas are mesenchymal malignancies of bone or soft tissues that can develop in different anatomic sites and distinct connective tissue types, showing a wide spectrum of clinical behaviors and biological activity patterns [1,2]. Sarcomas display a high level of heterogeneity, with 75% of them originating from soft tissue (STS), 15% of them being gastrointestinal stromal tumors (GIST), and 10% of them arising from bones (BS), comprising more than 170 distinct subtypes [3,4]. Sarcomas are rare neoplasms, constituting less than 1% of adult malignancies and 15% of non-hematologic childhood malignancies [3,4]. The mainstay of treatment of regional STS is surgery, while chemotherapy (CT) and radiotherapy (RT) may be used as neoadjuvant or adjuvant treatments [3]. In a metastatic setting,